Discussion

TCDD is a widespread environmental contaminant that influences several basic homeostatic control mechanisms in the body via AhR (3). T cells are a possible direct target for TCDD, as evidenced by the presence of the AhR in T cells, and inhibition of T cell growth by the expression of a constitutively active AhR mutant in AhR-null Jurkat T cells or following TCDD treatment (1, 41). It has been demonstrated that expression of AhR in both $CD4^+$ and $CD8^+$ T cells is required for a full suppression of an allospecific CTL response by TCDD, indicating a direct role for AhR in these TCDD-induced immunosuppressive effects (1, 42). However, the relationship between in vivo TCDD exposure and breakdown in T cell tolerance has not been well defined.

In this study, we demonstrated that neonatal exposure to low-dose TCDD could induce autoimmunity in the salivary glands using a NFS/*sld* strain associated with disease-susceptible autoantibody production, such as anti-SSA/La, anti-SSB/Ro, and anti-α-fodrin Abs. It has been reported that TCDD causes extensive damage to the thymus to suppress T cell-dependent immune responses in vivo, including delayed-type and contact hypersensitivity responses and the generation of CTL (4, 43, 44). By contrast, neonatal exposure to TCDD had little influence on thymic atrophy in our experiment in which low-dose (0.0486 ± 0.0088 to 8.37 ± 0.7 μg/kg) TCDD was administered into neonatal mice on days 0, 1, and 2 (body weight: 1.2 ± 0.1 to 2.1 ± 0.35 g) after birth. The dosage of TCDD was considerably lower than that in the experiments in which thymic atrophy or apoptosis was induced by in vivo exposure to TCDD (30–50 μg/kg) (31, 32). For instance, it was reported that 60% apoptotic cells of thymus were observed in normal mice injected with 50 μg/kg TCDD, whereas 20–30% apoptotic cells of thymus were observed in vehicle-injected mice. In addition, although the loss of mitochondrial membrane potential related to apoptosis of thymocytes was not detected in ~10 μg/kg TCDD-treated mice, the loss was observed in 10–50 μg/kg TCDD-treated mice (31). Thus, the exposure to low dosage under 10 μg/kg TCDD may have an influence on neonatal thymic differentiation or selection in NFS/*sld* mice, but not atrophy or apoptosis, to induce autoimmune disease as the late effect. Moreover, T cell proliferation by anti-CD3 and -CD28 mAbs and Th1-type cytokine production, such as IL-2 and IFN-γ from splenic $CD4^+$ T cells, were significantly more enhanced by neonatal TCDD treatment than those in control mice. These findings were consistent with the reports that TCDD enhances proliferation and cytokine production of mitogen- or Ag-stimulated T cells or T cell clones (1, 8). Because there were alterations in the percentage and number of DN cells in TCDD-treated mice, we analyzed this population using CD44 and CD25 markers. After TCDD treatment in this set, there was a decrease in the percentage of $CD44^+CD25^-$ cells (DN1) and $CD44^-CD25^-$ cells (DN4), and a relative increase in the percentage of $CD44^+CD25^+$ cells (DN2) and $CD44^-CD25^+$ cells (DN3). Analysis of the actual numbers of cells in each population compared with controls suggested that thymic maturation or negative selection at DN2 or DN3 might be affected by neonatal exposure to the low-dose TCDD. These results suggest that TCDD is interfering with the development and/or the proliferation of DN cells. Furthermore, the early stage of DN and the late stage into CD4SP or CD8SP in the thymic differentiation were disturbed by low-dose TCDD treatment, indicating that the immunotoxicity of TCDD on neonatal thymus might lead to the development of T cell-dependent autoimmunity. The inflammatory lesions were observed in the organs other than salivary gland including kidney, lung, and liver in TCDD-treated mice. Although the inflammatory lesions in liver, lung, and kidney from female mice treated with 10 ng of TCDD at 2 mo of age were observed, the severity of extraglandular lesions was lower than that of salivary gland, and the onset was later compared with that in salivary gland. Most of the extraglandular lesions of both female and male mice were developed with aging. We have previously demonstrated that the extraglandular lesion such as autoimmune arthritis in 3d-Tx NFS/*sld* mice was observed with aging (45, 46). Therefore, it is possible that TCDD may enhance any age-related reaction in the organs to induce autoimmunity.

In this study, there were no changes in the B cell number and proliferation in spleen from low-dose TCDD-treated mice, although the suppressive effect of the T cell-dependent Ab response to sheep RBC was reported in C57BL/6 mice injected with TCDD (47). In addition, TCDD selectively inhibited terminal B cell differentiation into plasma cells in response to trinitrophenol-LPS without altering early events in B cell activation or proliferation (48). By contrast, in our study significantly increased autoantibody productions such as anti-SSA/La, anti-SSB/Ro, and anti-α-fodrin were observed by neonatal exposure to low-dose TCDD. Although it is still unclear whether the direct or indirect effect of TCDD on B cells influences autoantibody production, this new finding may be a key to understand the association of TCDD immunotoxicity with the development of autoimmunity.

AhR is a cytoplasmic receptor protein and has been described as a ligand-activated transcription factor that mediates induction of xenobiotic metabolizing enzymes (27, 28, 49). Upon ligand binding, the AhR translocates into the nucleus and dimerizes with ARNT. The AhR/ARNT complex binds to specific gene promoter elements (50). In this study, significantly increased expressions of AhR mRNA and protein in neonatal thymus were observed compared with those in adult thymus. This suggests that neonatal exposure to low-dose TCDD may effect thymic differentiation and/or maturation through AhR by disrupting the T cell tolerance more intensively than those in adult thymus. If negative or positive selection in the neonatal thymus is disrupted by low-dose TCDD exposure, autoreactive T cells may be released to the periphery and expand in response to any autoantigen leading to induce autoimmunity. Increased expression of AhR mRNA and the disrupted thymic differentiation in the neonatal thymus by low-dose TCDD exposure may support this hypothesis.

CYP1A1 is known to have pivotal roles in cell growth and apoptosis (51, 52). In the present study, CYP1A1 mRNA of neonatal thymocytes was readily up-regulated by TCDD, whereas the expression of adult thymocytes was constant in the response to TCDD. Neonatal exposure to low-dose TCDD may influence proliferation, differentiation, or apoptosis of thymocytes through CYP1A1 at early stages, such as DN. Namely, it is possible that negative selection leading cell apoptosis at DN3 might be disturbed by neonatal exposure to TCDD. As a result, autoreactive T cells leaking from thymic selection might survive and proliferate in response to any autoantigen in the periphery, leading to the induction of autoimmune lesions. The activation of AhR by TCDD results in an increased binding activity to NF-κB subunit RelB of AhR itself to form AhR/RelB complex, which was associated with an increased mRNA level of multiple inflammatory genes (53). Overexpression of AhR and RelB led to an increased level of CCL1 and IRF-3 in control as well as TCDD-stimulated cells supporting the role of RelB and AhR for the transcriptional regulation of these genes (54). In the present study, TCDD enhanced TCR-mediated classical NF-κB activation of neonatal thymocytes from NFS/*sld* mice more than adult thymocytes. In addition, some NF-κB-target genes such as Bcl-x_L and TNF-α in thymus were up-regulated by in vivo TCDD injection. Our data demonstrate that

TCDD/AhR signal may influence the differentiation or development of T cells in the neonatal thymus associated with autoimmunity. However, the precise mechanism of how the NF-κB activation, including classical and nonclassical pathway, interacts with TCDD/AhR signal is still unclear.

It has been well known that autoimmune lesions of multiple organs such as lacrimal glands, salivary glands, pancreas, and liver are observed in AIRE gene-deficient mice (39). AIRE was reported to play a pivotal role in the expression of tissue-specific autoantigens such as salivary protein-1, GAD67, insulin, or other self-proteins in the TECs that express the MHC class II on the cell surface and function as APCs to immature T cells for the immunological selection of central tolerance in the thymus (55). In this study, mRNA expressions of AIRE and tissue-specific autoantigens such as salivary protein-1 and GAD67 in the thymus were reduced by the in vivo neonatal exposure to low-dose TCDD in NFS/*sld* mice. The finding indicated that TCDD might influence the selection of autoreactive T cells in the thymus through AIRE. There may be any complex molecular mechanisms related to the avidity of TCR, haplotype of MHC class II, Ag-specificity, T cell apoptosis, interaction with TEC, or TCDD signal.

The AhR has been shown to mediate various immunotoxic responses induced by environmental pollutants like TCDD (56). Although our results show that activation of the AhR by TCDD effects T cell development, the receptor does not seem to play a key role in the establishment of a normal T cell compartment. The AhR has been shown to play important roles in regulating the expression of several cytokines. For example, exposure of rats to TCDD led to up-regulation of IL-1β and TNF-α in the liver (57, 58). Interestingly, although TCDD suppressed the production of IFN-γ by mediastinal lymph node cells, there was a 10-fold increase in the IFN-γ level in the lungs of TCDD-treated mice (59). Autoimmune disease is caused by heterogeneous etiology, involving interplay between predisposing genes and triggering environmental factors. Although a lot of studies have demonstrated the immunotoxicity of TCDD, this study is the first to induce autoimmunity by neonatal low-dose TCDD treatment. Recently it has been reported that AhR links T_H17 cell-mediated experimental autoimmune encephalomyelitis to environmental toxins through altering the differentiation of Treg cells (60, 61). The low-dose TCDD exposure in our model had little influence on the number of Treg cells in spleen and the function of T_H17 cells, such as IL-17 production from T cells. The action of TCDD via AhR may influence peripheral tolerance related to autoimmunity besides central tolerance in thymus.

Taken together, our new findings may explain the risk for autoimmunity caused by the late effect of early exposure to environmental pollution, including TCDD. And as shown here, our model would help to understand the multifactorial nature of autoimmune disease.

Acknowledgments

We thank Ai Nagaoka, Noriko Kino, Risa Okada, Ritsuko Oura, and Satoko Yoshida for technical assistance.

Disclosures

The authors have no financial conflict of interest.

References

1. Kerkvliet, N. I. 2001. Recent advances in understanding the mechanisms of TCDD immunotoxicity. *Int. Immunopharmacol.* 2: 277–291.
2. Wormley, D. D., A. Ramesh, and D. B. Hood. 2004. Environmental contaminant-mixture effects on CNS development, plasticity, and behavior. *Toxicol. Appl. Pharmacol.* 197: 49–65.
3. Schecter, A., L. Birnbaum, J. J. Ryan, and J. D. Constable. 2006. Dioxins: an overview. *Environ. Res.* 101: 419–428.
4. Laiosa, M. D., A. Wyman, F. G. Murante, N. C. Fiore, J. E. Staples, T. A. Gasiewicz, and A. E. Silverstone. 2003. Cell proliferation arrest within intrathymic lymphocyte progenitor cells causes thymic atrophy mediated by the aryl hydrocarbon receptor. *J. Immunol.* 171: 4582–4591.
5. Gehrs, B. C., and R. J. Smialowicz. 1999. Persistent suppression of delayed-type hypersensitivity in adult F344 rats after perinatal exposure to 2,3,7,8-tetrachlorodibenzo-p-dioxin. *Toxicology* 134: 79–88.
6. Walker, D. B., W. C. Williams, C. B. Copeland, and R. J. Smialowicz. 2004. Persistent suppression of contact hypersensitivity, and altered T-cell parameters in F344 rats exposed perinatally to 2,3,7,8-tetrachlorodibenzo-*p*-dioxin (TCDD). *Toxicology* 197: 57–66.
7. Prell, R. A., E. Dearstyne, L. G. Steppan, A. T. Vella, and N. I. Kerkvliet. 2000. CTL hyporesponsiveness induced by 2,3,7,8-tetrachlorodibenzo-*p*-dioxin: role of cytokines and apoptosis. *Toxicol. Appl. Pharmacol.* 166: 214–221.
8. Prell, R. A., J. A. Oughton, and N. I. Kerkvliet. 1995. Effect of 2,3,7,8-tetrachlorodibenzo-*p*-dioxin on anti-CD3-induced changes in T-cell subsets and cytokine production. *Int. J. Immunopharmacol.* 17: 951–961.
9. Shepherd, D. M., E. A. Dearstyne, and N. I. Kerkvliet. 2000. The effects of TCDD on the activation of ovalbumin (OVA)-specific DO11.10 transgenic CD4(+) T cells in adoptively transferred mice. *Toxicol. Sci.* 56: 340–350.
10. Morris, D. L., J. G. Karras, and M. P. Holsapple. 1993. Direct effects of 2,3,7,8-tetrachlorodibenzo-p-dioxin (TCDD) on responses to lipopolysaccharide (LPS) by isolated murine B-cells. *Immunopharmacology* 26: 105–112.
11. Karras, J. G., and M. P. Holsapple. 1994. Inhibition of calcium-dependent B cell activation by 2,3,7,8-tetrachlorodibenzo-*p*-dioxin. *Toxicol. Appl. Pharmacol.* 125: 264–270.
12. Dooley, R. K., D. L. Morris, and M. P. Holsapple. 1990. Elucidation of cellular targets responsible for tetrachlorodibenzo-p-dioxin (TCDD)-induced suppression of antibody responses. II. The role of the T-lymphocyte. *Immunopharmacology* 19: 47–58.
13. Gotter, J., and B. Kyewski. 2004. Regulating self-tolerance by deregulating gene expression. *Curr. Opin. Immunol.* 16: 741–745.
14. Anderton, S., C. Burkhart, B. Metzler, and D. Wraith. 1999. Mechanisms of central and peripheral T-cell tolerance: lessons from experimental models of multiple sclerosis. *Immunol. Rev.* 169: 123–127.
15. Miller, J. F., and R. A. Flavell. 1994. T-cell tolerance and autoimmunity in transgenic models of central and peripheral tolerance. *Curr. Opin. Immunol.* 6: 892–899.
16. Kruize, A. A., R. J. Sweenk, and L. Kater. 1995. Diagnostic criteria and immunopathogenesis of Sjögren's syndrome: implications for therapy. *Immunol. Today* 16: 557–559.
17. Fox, R. I., M. Stern, and P. Michelson. 2000. Update in Sjögren syndrome. *Curr. Opin. Rheumatol.* 12: 391–398.
18. Fox, R. I. 2005. Sjögren's syndrome. *Lancet* 366: 321–331.
19. Haneji, N., H. Hamano, K. Yanagi, and Y. Hayashi. 1994. A new animal model for primary Sjögren's syndrome in NFS/*sld* mutant mice. *J. Immunol.* 153: 2769–2777.
20. Haneji, N., T. Nakamura, K. Takio, K. Yanagi, H. Higashiyama, I. Saito, S. Noji, H. Sugino, and Y. Hayashi. 1997. Identification of α-fodrin as a candidate autoantigen in primary Sjögren's syndrome. *Science* 275: 604–607.
21. Saegusa, K., N. Ishimaru, K. Yanagi, K. Mishima, R. Arakaki, T. Suda, I. Saito, and Y. Hayashi. 2002. Prevention and induction of autoimmune exocrinopathy is dependent on pathogenic autoantigen cleavage in murine Sjögren's syndrome. *J. Immunol.* 169: 1050–1057.
22. Suri-Payer, E., K. Wei, and K. Tung. 2001. The day-3 thymectomy model for induction of multiple organ-specific autoimmune diseases. *Curr. Protoc. Immunol.* 15: 15–16.
23. Kojima, A., Y. Tanaka-Kojima, T. Sakakura, and Y. Nishizuka. 1976. Spontaneous development of autoimmune thyroiditis in neonatally thymectomized mice. *Lab. Invest.* 34: 550–557.
24. Teague, P. O., E. J. Yunis, G. Rodey, A. J. Fish, O. Stutman, and R. A. Good. 1970. Autoimmune phenomena and renal disease in mice: role of thymectomy, aging, and involution of immunologic capacity. *Lab. Invest.* 22: 121–130.
25. Tung, K. S., S. Smith, P. Matzner, K. Kasai, J. Oliver, F. Feuchter, and R. E. Anderson. 1987. Murine autoimmune oophoritis, epididymoorchitis, and gastritis induced by day 3 thymectomy. *Am. J. Pathol.* 126: 303–314.
26. Safe, S. 2001. Molecular biology of the Ah receptor and its role in carcinogenesis. *Toxicol. Lett.* 120: 1–7.
27. Denison, M. S., and S. Heath-Pagliuso. 1998. The Ah receptor: a regulator of the biochemical and toxicological actions of structurally diverse chemicals. *Bull. Environ. Contam. Toxicol.* 61: 557–568.
28. Marlowe, J. L., and A. Puga. 2005. Aryl hydrocarbon receptor, cell cycle regulation, toxicity, and tumorigenesis. *J. Cell. Biochem.* 96: 1174–1184.
29. Nohara, K., H. Fujimaki, S. Tsukumo, K. Inouye, H. Sone, and C. Tohyama. 2002. Effects of 2,3,7,8-tetrachlorodibenzo-*p*-dioxin (TCDD) on T cell-derived cytokine production in ovalbumin (OVA)-immunized C57Bl/6 mice. *Toxicology* 172: 49–58.
30. Neff-LaFord, H. D., B. A. Vorderstrasse, and B. P. Lawrence. 2003. Fewer CTL, not enhanced NK cells, are sufficient for viral clearance from the lungs of immunocompromised mice. *Cell. Immunol.* 226: 54–64.
31. Tomita, S., H. B. Jiang, T. Ueno, S. Takagi, K. Tohi, S. Maekawa, A. Miyatake, A. Furukawa, F. J. Gonzalez, J. Takeda, T. Ichikawa, and Y. Takahama. 2003. T cell-specific disruption of arylhydrocarbon receptor nuclear translocator (Arnt) gene causes resistance to 2,3,7,8-tetrachlorodibenzo-*p*-dioxin-induced thymic involution. *J. Immunol.* 171: 4113–4120.
32. Camacho, I. A., N. Singh, V. L. Hegde, M. Nagarkatti, and P. S. Nagarkatti. 2005. Treatment of mice with 2,3,7,8-tetrachlorodibenzo-*p*-dioxin leads to aryl

hydrocarbon receptor-dependent nuclear translocation of NF-κB and expression of Fas ligand in thymic stromal cells and consequent apoptosis in T cells. *J. Immunol.* 175: 90–103.
33. White, S. C., and G. W. Casarett. 1974. Induction of experimental autoallergic sialadenitis. *J. Immunol.* 112: 178–185.
34. Kohashi, M., N. Ishimaru, R. Arakaki, and Y. Hayashi. 2008. Effective treatment with oral administration of rebamipide in a mouse model for Sjogren's syndrome. *Arthritis Rheum.* 58: 389–400.
35. Rengarajan, J., S. J. Szabo, and L. H. Glimcher. 2000. Treanscriptional regulation oh Th1/Th2 polarization. *Immunol. Today* 21: 479–783.
36. Riddick, D. S., Y. Huang, P. A. Harper, and A. B. Okey. 1994. 2,3,7,8-Tetrachlorodibenzo-*p*-dioxin versus 3-methylcholanthrene: comparative studies of Ah receptor binding, transformation, and induction of CYP1A1. *J. Biol. Chem.* 269: 12118–12128.
37. Singh, N. P., M. Nagarkatti, and P. S. Nagarkatti. 2007. Role of dioxin response element and nuclear factor-κB motifs in 2,3,7,8-tetrachlorodibenzo-*p*-dioxin-mediated regulation of Fas and Fas ligand expression. *Mol. Pharmacol.* 71: 145–157.
38. Bonizzi, G., and M. Karin. 2004. The two NF-κB activation pathways and their role in innate and adaptive immunity. *Trends Immunol.* 25: 280–288.
39. Anderson, M. S., E. S. Venanzi, L. Klein, Z. Chen, S. P. Berzins, S. J. Turley, H. von Boehmer, R. Bronson, A. Dierich, C. Benoist, and D. Mathis. 2002. Protection of an immunological self shadow within the thymus by the aire protein. *Science* 298: 1395–1401.
40. Kuroda, N., T. Mitani, N. Takeda, N. Ishimaru, R. Arakaki, Y. Hayashi, Y. Bando, K. Izumi, T. Takahashi, T. Nomura, et al. 2005. Development of autoimmunity against transcriptionally unrepressed target antigen in the thymus of Aire-deficient mice. *J. Immunol.* 174: 1862–1870.
41. Ito, T., S. Tsukumo, N. Suzuki, H. Motohashi, M. Yamamoto, Y. Fujii-Kuriyama, J. Mimura, T. M. Lin, R. E. Peterson, C. Tohyama, and K. Nohara. 2004. A constitutively active arylhydrocarbon receptor induces growth inhibition of Jurkat T cells through changes in the expression of genes related to apoptosis and cell cycle arrest. *J. Biol. Chem.* 279: 25204–25210.
42. Nagarkatti, P. S., G. D. Sweeney, J. Gauldie, and D. A. Clark. 1984. Sensitivity to suppression of cytotoxic T cell generation by 2,3,7,8-tetrachlorodibenzo-*p*-dioxin (TCDD) is dependent on the Ah genotype of the murine host. *Toxicol. Appl. Pharmacol.* 72: 169–176.
43. Nohara, K., X. Pan, S. Tsukumo, A. Hida, T. Ito, H. Nagai, K. Inouye, H. Motohashi, M. Yamamoto, Y. Fujii-Kuriyama, and C. Tohyama. 2005. Constitutively active aryl hydrocarbon receptor expressed specifically in T-lineage cells causes thymus involution and suppresses the immunization-induced increase in splenocytes. *J. Immunol.* 174: 2770–2777.
44. Staples, J. E., F. G. Murante, N. C. Fiore, T. A. Gasiewicz, and A. E. Silverstone. 1998. Thymic alterations induced by 2,3,7,8-tetrachlorodibenzo-*p*-dioxin are strictly dependent on aryl hydrocarbon receptor activation in hemopoietic cells. *J. Immunol.* 160: 3844–3854.
45. Ishimaru, N., T. Yoneda, K. Saegusa, K. Yanagi, N. Haneji, K. Moriyama, I. Saito, and Y. Hayashi. 2000. Severe destructive autoimmune lesions with aging in murine Sjögren's syndrome through Fas-mediated apoptosis. *Am. J. Pathol.* 156: 1557–1564.
46. Kobayashi, M., N. Yasui, N. Ishimaru, R. Arakaki, and Y. Hayashi. 2004. Development of autoimmune arthritis with aging via bystander T cell activation in the mouse model of Sjögren's syndrome. *Arthritis Rheum.* 50: 3974–3984.
47. Kerkvliet, N. I., and J. A. Brauner. 1987. Mechanisms of 1,2,3,4,6,7,8-heptachlorodibenzo-*p*-dioxin (HpCDD)-induced humoral immune suppression: evidence of primary defect in T-cell regulation. *Toxicol. Appl. Pharmacol.* 87: 47–58.
48. Luster, M. I., D. R. Germolec, G. Clark, G. Wiegand, and G. J. Rosenthal. 1998. Selective effects of 2,3,7,8-tetrachlorodibenzo-*p*-dioxin and corticosteroid on in vitro lymphocyte maturation. *J. Immunol.* 140: 928–935.
49. Schmidt, J. V., G. H. Su, J. K. Reddy, M. C. Simon, and C. A. Bradfield. 1996. Characterization of a murine Ahr null allele: involvement of the Ah receptor in hepatic growth and development. *Proc. Natl. Acad. Sci. USA* 93: 6731–6736.
50. Gu, Y. Z., J. B. Hogenesch, and C. A. Bradfield. 2000. The PAS superfamily: sensors of environmental and developmental signals. *Annu. Rev. Pharmacol. Toxicol.* 40: 519–561.
51. Umannova, L., J. Zatloukalova, M. Machala, P. Krcmar, Z. Majkova, B. Hennig, A. Kozubik, and J. Vondracek. 2007. Tumor necrosis factor-α modulates effects of aryl hydrocarbon receptor ligands on cell proliferation and expression of cytochrome P450 enzymes in rat liver "stem-like" cells. *Toxicol. Sci.* 99: 79–89.
52. Hoagland, M. S., E. Hoagland, and H. I. Swanson. 2005. The p53 inhibitor pifithrin-α is a potent agonist of aryl hydrocarbon receptor. *J. Pharmacol. Exp. Ther.* 314: 603–610.
53. Vogel, C. F., E. Sciullo, W. Li, P. Wong, G. Lazennec, and F. Matsumura. 2007. RelB, a new partner of aryl hydrocarbon receptor-mediated transcription. *Mol. Endocrinol.* 21: 2941–2955.
54. Vogel, C. F., E. Sciullo, and F. Matsumura. 2007. Involvement of RelB in aryl hydrocarbon receptor-mediated induction of chemokines. *Biochem. Biophys. Res. Commun.* 363: 722–726.
55. Gillard, G. O., and A. G. Farr. 2005. Contrasting models of promiscuous gene expression by thymic epithelium. *J. Exp. Med.* 202: 15–19.
56. Mandal, P. K. 2005. Dioxin: a review of its environmental effects and its aryl hydrocarbon receptor biology. *J. Comp. Physiol.* 175: 221–230.
57. Fan, F., B. Yan, G. Wood, M. Viluksela, and K. K. Rozman. 1997. Cytokines (IL-1β and TNFα) in relation to biochemical and immunological effects of 2,3,7,8-tetrachlorodibenzo-*p*-dioxin (TCDD) in rats. *Toxicology* 116: 9–16.
58. Vogel, C., S. Donat, O. Döhr, L. Kremer, C. Esser, M. Roller, and J. Abel. 1997. Effect of subchronic 2,3,7,8-tetrachlorodibenzo-*p*-dioxin exposure on immune system and target gene responses in mice: calculation of benchmark doses for CYP1A1 and CYP1A2 related enzyme activities. *Arch. Toxicol.* 71: 372–382.
59. Warren, T. K., K. A. Mitchell, and B. P. Lawrence. 2000. Exposure to 2,3,7,8-tetrachlorodibenzo-*p*-dioxin (TCDD) suppresses the humoral and cell-mediated immune responses to influenza A virus without affecting cytolytic activity in the lung. *Toxicol. Sci.* 56: 114–123.
60. Veldhoen, M., K. Hirota, A. M. Westendorf, J. Buer, L. Dumoutier, J. C. Renauld, and B. Stockinger. 2008. The aryl hydrocarbon receptor links TH17-cell-mediated autoimmunity to environmental toxins. *Nature* 453: 106–110.
61. Quintana, F. J., A. S. Basso, A. H. Iglesias, T. Korn, M. F. Farez, E. Bettelli, M. Caccamo, M. Oukka, and H. L. Weiner. 2008. Control of Treg and TH17 cell differentiation by the aryl hydrocarbon receptor. *Nature* 453: 65–72.

Structure-Activity–Dependent Regulation of Cell Communication by Perfluorinated Fatty Acids using *in Vivo* and *in Vitro* Model Systems

Brad L. Upham,[1] Joon-Suk Park,[1] Pavel Babica,[1] Iva Sovadinova,[1] Alisa M. Rummel,[1] James E. Trosko,[1] Akihiko Hirose,[2] Ryuichi Hasegawa,[2] Jun Kanno,[3] and Kimie Sai[3**]*

[1]Department of Pediatrics and Human Development, National Food Safety and Toxicology Center, Michigan State University, East Lansing, Michigan, USA; [2]Division of Risk Assessment, and [3]Division of Cellular and Molecular Toxicology, National Institute of Health Sciences, Tokyo, Japan

BACKGROUND: Perfluoroalkanoates, [e.g., perfluorooctanoate (PFOA)], are known peroxisome proliferators that induce hepatomegaly and hepatocarcinogenesis in rodents, and are classic nongenotoxic carcinogens that inhibit *in vitro* gap-junctional intercellular communication (GJIC). This inhibition of GJIC is known to be a function of perfluorinated carbon lengths ranging from 7 to 10.

OBJECTIVES: The aim of this study was to determine if the inhibition of GJIC by PFOA but not perfluoropentanoate (PFPeA) observed in F344 rat liver cells *in vitro* also occurs in F344 rats *in vivo* and to determine mechanisms of PFOA dysregulation of GJIC using *in vitro* assay systems.

METHODS: We used an incision load/dye transfer technique to assess GJIC in livers of rats exposed to PFOA and PFPeA. We used *in vitro* assays with inhibitors of cell signaling enzymes and antioxidants known to regulate GJIC to identify which enzymes regulated PFOA-induced inhibition of GJIC.

RESULTS: PFOA inhibited GJIC and induced hepatomegaly in rat livers, whereas PFPeA had no effect on either end point. Serum biochemistry of liver enzymes indicated no cytotoxic response to these compounds. *In vitro* analysis of mitogen-activated protein kinase (MAPK) indicated that PFOA, but not PFPeA, can activate the extracellular receptor kinase (ERK). Inhibition of GJIC, *in vitro*, by PFOA depended on the activation of both ERK and phosphatidylcholine-specific phospholipase C (PC-PLC) in the dysregulation of GJIC in an oxidative-dependent mechanism.

CONCLUSIONS: The *in vitro* analysis of GJIC, an epigenetic marker of tumor promoters, can also predict the *in vivo* activity of PFOA, which dysregulated GJIC via ERK and PC-PLC.

KEY WORDS: extracellular receptor kinase, gap-junctional intercellular communication, mitogen-activated protein kinase, perfluorooctanoate, perfluoropentanoate, phosphatidylcholine-specific-phospholipase C, tumor promotion. *Environ Health Perspect* 117:545–551 (2009). doi:10.1289/ehp.11728 available via *http://dx.doi.org/* [Online 23 October 2008]

Research on the environmental fate and toxicology of halogenated compounds has focused primarily on brominated and chlorinated organics, whereas fluorinated organics received less attention, partly because of the perception that these compounds, which are quite chemically inert, were also biologically inert (Key et al. 1997). However, perfluorinated fatty acids (PFFAs), such as perfluorooctanoate (PFOA) and perfluorooctane sulfonate (PFOS), are found in the environment and have been detected in the blood of animals throughout the world, including the seals of remote arctic regions, indicating widespread distribution (Kannan 2001; Tao 2006; Van de Vijver 2005). Significant levels of PFOA and PFOS have also been detected in the serum of humans, but there is evidence of a significant decline in body burdens of PFOS and PFOA over the last 5–10 years (Calafat et al. 2007). The values from the first National Health and Nutrition Examination Survey (NHANES) conducted from 1999 to 2000 reported geometric means of 30.4 μg PFOS/L and 5.4 μg PFOA/L, and the second NHANES conducted between 2003 and 2004 reported geometric means of 20.7 μg PFOS/L and 3.9 μg PFOA/L (Calafat et al. 2007). Contamination of the environment is not limited to PFOA and PFOS but also includes short-chain perfluorinated alkanoates, such as perfluorobutyrate, perfluoropentanoate (PFPeA), perfluorohexanoate, and perfluoroheptanoate (Skutlarek et al. 2006).

The acute toxicities of PFOA and PFOS in rodent systems are low (Hekster 2003; Kudo and Kawashima 2003). After the absorption of PFOA into the body, it is predominantly distributed in the liver and plasma and, to a lesser extent, the kidney and lungs (Kudo and Kawashima 2003). Thus, the chronic and short-term effects of PFOA in rats are found largely in the liver (Kennedy et al. 2004) and immune system (DeWitt et al. 2008). Peroxisome proliferation in rodent livers is one of the major responses to PFOA, along with subsequent interferences with normal metabolism of fatty acids and cholesterol, and the induction of hepatocellular hypertrophy (Kennedy et al. 2004). Peroxisome-proliferating chemicals are classic nongenotoxic tumor promoters in rodent liver tissue (Cattley et al. 1995), and like other peroxisome proliferators, PFOA has also been shown to strongly promote tumors in rodent livers (Abdellatif et al. 1991). However, peroxisome-proliferating compounds might not be strong tumor promoters in human livers because of species differences in the response to peroxisome proliferators *in vivo*, with rodents more responsive than primates (Klaunig et al. 2003).

Although the underlying mechanisms of tumor promotion might vary, such as the induction of peroxisome proliferation, tumorigenic cells have long been characterized as cells that lose their ability to regulate growth through contact inhibition (Borek and Sachs 1966) and lack the ability to terminally differentiate (Potter 1978), which implies a breakdown in one of the communicating mechanisms (Trosko and Upham 2005). Tumorigenic cells can be benign, leading to the compression of surrounding tissues, or have the potential to acquire genetic mutations that lead to a malignant state where the cancerous cells can invade surrounding tissues. Alteration of cell-to-cell communication via gap junctions has been implicated in the tumorigenic process and is supported by considerable evidence (Trosko and Ruch 2002).

Inhibition of gap-junctional intercellular communication (GJIC) appears to be a necessary, albeit insufficient, step of tumorigenesis and is therefore a common response of cells to tumor promoters, oncogenes, growth factors, and nongenotoxic carcinogens such as peroxisome proliferators (Trosko and Ruch 1998; Trosko and Upham 2005). Although GJIC is modulated by multiple signaling pathways, simple bioassays of intercellular communication can be used to assess dysregulation of gap junctions regardless of the upstream effectors.

Address correspondence to B.L. Upham, Michigan State University, 243 National Food Safety and Toxicology Center, East Lansing, MI 48824 USA. Telephone: (517) 884-2051. Fax: (517) 432-6340. E-mail: upham@msu.edu

*Current address: Division of Medical Safety Science, National Institute of Health Sciences, Tokyo, Japan.

**Current address: Division of Functional Biochemistry and Genomics, National Institute of Health Sciences, Tokyo, Japan.

This research was supported by National Institute of Environmental Health Sciences (NIEHS) grant R01 ES013268-01A2 to B.L.U. and by a Grant-in-Aid for Science Research from the Ministry of Education, Science, Sports, and Culture of Japan (11694334).

The contents of this article are solely the responsibility of the authors and do not necessarily represent the official views of the NIEHS.

The authors declare they have no competing financial interests.

Received 23 May 2008; accepted 23 October 2008.

Thus, GJIC is an excellent biomarker first to assess the potential tumorigenicity of chemicals and then to use as a cell signaling end point to determine the early molecular events induced by these chemicals.

Cell proliferative diseases, such as cancer, not only require the release of a quiescent cell from growth suppression via down-regulation of GJIC and/or changes in extracellular components (i.e., integrins), but also need to activate mitogenic signaling pathways. The mitogen-activated protein kinase (MAPK) pathways are the major intracellular signaling mechanisms by which a cell activates, via phosphorylation, transcription factors involved in mitogenesis (Denhardt 1996). The extracellular receptor kinase (ERK) pathway has been extensively characterized, is the most understood of the MAPK pathways (Denhardt 1996), and is a key pathway of carcinogenesis (Roberts and Der 2007).

In the present study, we extended our *in vitro* studies with F344 rat liver epithelial cells, which determined that PFOA, but not PFPeA, inhibited GJIC (Upham et al. 1998), to an *in vivo* study using F344 rats exposed to PFOA, PFPeA, or phenobarbital (PB), a known tumor promoter, to determine GJIC in liver tissue. We also continued our *in vitro* studies of PFOA versus PFPeA in determining differential effects of these compounds on MAPK, specifically ERK, and further determined that the mechanism of PFOA-induced inhibition of GJIC depends on redox activity, ERK, and phosphatidylcholine-specific phospholipase C (PC-PLC).

Materials and Methods

Chemicals. We purchased PFOA (purity > 90%) and PFPeA (purity = 97%), for the data presented in Figures 1–3 and 4A, from Fluka Chemie AG (Buchs, Switzerland), and because of unavailability from Fluka, we purchased PFOA for the data presented in Figures 4B, 5, and 6 from Aldrich Chemical Company Inc. (Milwaukee, WI, USA), with a purity of 96%. The purity values were obtained from the commercial sources. The ratios of linear versus branched isomers in our samples were undetermined. The stock solutions were prepared by dissolving the powder in the solvent: acetonitrile for the *in vitro* assays and dimethyl sulfoxide (DMSO) for the *in vivo* studies; we also used these solvents as the vehicle controls. We purchased Lucifer yellow (LY) from Molecular Probes (Eugene, OR, USA); sodium dodecyl sulfate, Tween 20, Tris, glycine, acrylamide, tetramethylethylenediamine (TEMED) and DC protein kit from Bio-Rad Laboratories (Hercules, CA, USA); DMSO, rhodamine-dextran (RhD; molecular weight, 10,000 Da), dithiothreitol (DTT), *N*-acetylcysteine (Nac), L-ascorbate-2-phosphate (Asc-2-P) sesquimagnesium salt hydrate, and PB from Sigma-Aldrich Chemical Company (St. Louis, MO, USA); D609 and U0126, from Tocris Bioscience (Ellisville, MO, USA); resveratrol from CTMedChem (Bronx, NY, USA); acetonitrile, from EM Science (Gibstown, NJ, USA); polyclonal antibodies directed to phospho-ERK, from New England Biolabs (Ipswich, MA, USA); and mouse polyclonal antibody directed to glyceraldehyde 3-phosphate dehydrogenase (GAPDH), from Chemicon (Temecula, CA, USA).

In vivo *study*. Animal treatment. The protocol for this study was approved by the Animal Care and Utilization Committee of the National Institutes of Health Sciences of Japan to assure that the rats were treated humanely and with regard for alleviation of suffering. Male Fischer-344 (F344) rats, 5 weeks old, were purchased from Charles River Japan (Kanagawa, Japan) and housed in plastic cages (five rats/cage). Male F-344 rats were chosen to match the *in vitro* studies that used liver epithelial cells isolated from male F-344 rats. The rats were kept under conditions of controlled temperature (23 ± 2°C), humidity (55 ± 5%), and lighting (12/12-hr dark/light cycle) and given CRF-12 basal diet (Oriental Yeast Co., Tokyo, Japan) and tap water *ad libitum*.

We used the rats in the experiments after 1 week of acclimation. Eighty rats were divided into four groups and twenty rats per group were treated with a single intraperitoneal (i.p.) administration of 100 mg/kg PFOA, 100 mg/kg PFPeA, 100 mg/kg PB, or only vehicle (DMSO). Four rats per group were killed under anesthesia at 1, 3, 6, 12, and 24 hr after administration. Another 16 rats were divided into four groups and four rats of each group were given powder diet containing PFOA, PFPeA, PB, or basal powder diet only (control), and then killed after 1 week. The diets were prepared by blending each chemical into the basal powder diet at final concentrations of 0.02% for PFOA and PFPeA and 0.05% for PB. We determined the weight of the rats at the beginning and end of the experiment, and the food consumption on days 3 and 7 of the experiment. Based on the average weight of the rats and the average food consumed per day, the estimated daily doses of chemical exposures for PFOA, PFPeA, and PB were 37.9, 32.3, and 93.3 mg/day/kg, respectively.

Diethyl ether was used to euthanize the rats. Before sacrifice, blood was collected from the orbital venous plexus under anesthesia with diethyl ether and prepared for measuring serum aspartate aminotransferase (sAST), serum alanine aminotransferase (sALT), and serum alkaline phosphatase (sALP). Determination of sAST, sALT, and sALP was carried out with a Hitachi automatic Analyzer 7150 (Hitachi, Ltd., Tokyo, Japan) using commercially available GOP, GPT and ALP diagnostic reagents (Wako Pure Chemical Industries, Ltd., Tokyo, Japan). After opening the abdominal cavity, we excised the liver and immediately used one part of the liver for the incision loading/dye transfer (IL/DT). Our preliminary study confirmed that the anesthetic and the vehicle, DMSO, under our experimental conditions did not affect *in vivo* GJIC.

Bioassay of GJIC (IL/DT). We assayed *ex vivo* GJIC in the liver by the IL/DT method described previously (Sai et al. 2000). A part of the left lobe of the liver was put on a plastic

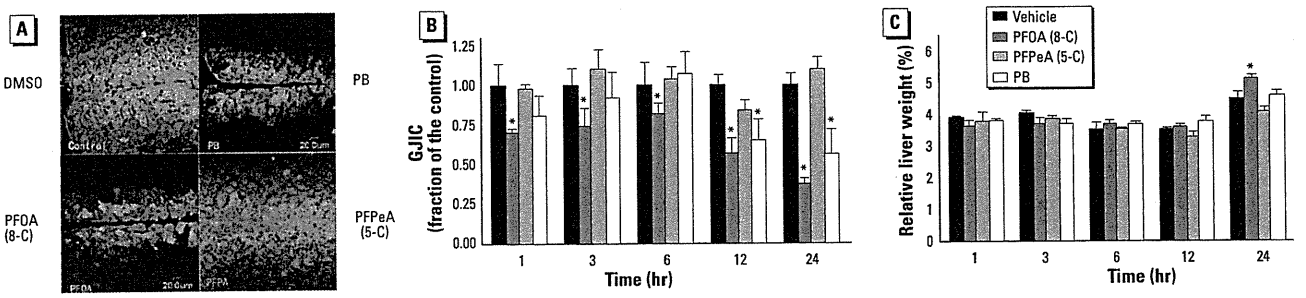

Figure 1. Analysis of *in vivo* effects of PFOA and PFPeA on GJIC in the liver tissue using IL/DT technique. Abbreviations: 5-C, five carbon; 8-C, eight carbon. (*A*) A fluorescent image of an IL/DT analysis of GJIC in the liver tissue of rats at 24 hr after a single i.p. administration of DMSO (vehicle), PB, PFOA, or PFPeA. Bar = 20 μm. (*B*) Mean + SD of the IL/DT data from rats treated with DMSO, PB, PFOA, or PFPeA for the acute exposure group. (*C*) Mean + SD relative liver weight from rats treated with DMSO, PB, PFOA, and PFPeA for the acute exposure group.

*$p < 0.05$ compared with vehicle, determined by one-way ANOVA for each time group followed by Dunnett's post hoc test.

plate covered with wet gauze. A mixture of fluorescent dyes containing 0.5 mg/mL LY and 0.5 mg/mL RhD in phosphate-buffered saline (PBS) was dropped on the tissue's surface. Three to four incisions were made on the surface of each specimen with a sharp blade. Excess amount of dye mixture was additionally put into the incisions and kept there for 3 min at room temperature. After incubation, the tissue was washed with PBS three times and fixed in 10% phosphate-buffered formalin overnight. Slices were washed with water and processed for embedding in paraffin. Five μm sections for GJIC analysis were prepared by cutting the paraffin block perpendicular to the incision line. Areas stained with LY alone or with RhD were detected by the emission of fluorescence using a confocal microscope (Fluoview, Olympus, Tokyo, Japan). We counted the number of cells stained with LY alone and normalized this number by dividing by the incision length. At least three incision sites per specimen were randomly chosen for the analysis, and the mean value was used as data from one animal. The values were expressed as a fraction of the control.

In vitro *study*. Cell culture. We obtained the WB-F344 rat liver epithelial cell line from J.W. Grisham and M.S. Tsao of the University of North Carolina at Chapel Hill, Chapel Hill, NC, USA (Tsao et al. 1984). Cells were cultured in D-medium (formula 78-5470EF, Gibco Laboratories, Grand Island, NY, USA), supplemented with 5% fetal bovine serum (Gibco Laboratories), and incubated at 37°C in a humidified atmosphere containing 5% CO_2 and 95% air. The cells were grown in 35-mm tissue culture plates (Corning Inc., Corning, NY, USA) and the culture medium was changed every other day. Bioassays were conducted with confluent cultures that were obtained after 2–3 days of growth.

These WB cells are diploid and nontumorigenic (Tsao et al. 1984) and have been extensively characterized for GJIC in the absence and presence of well-known tumor promoters, growth factors, tumor suppressor genes, and oncogenes (Trosko and Ruch 1998). Intrahepatic transplantation of WB cells, which are liver bipolar stem cells, into adult syngenic F344 rats results in the morphologic differentiation of these cells into hepatocytes and incorporation into hepatic plates (Coleman et al. 1993).

Bioassay of GJIC (scrape load/dye transfer). The scrape loading/dye transfer (SL/DT) technique was adapted after the method of Upham et al. (1998). The test chemicals were added directly to the cell culture medium from concentrated stock solutions. The migration of the dye through gap junctions was visualized with a Nikon Eclipse TE3000 phase contrast/fluorescent microscope and the images were digitally captured with Nikon EZ Cool Snap charge-coupled device camera (Nikon Inc., Nikon, Japan). GJIC was assessed by comparing the distance the dye traveled in the chemically treated cells with the distance the dye traveled in the vehicle controls, which was measured using the Gel-Expert imaging software (Nucleotech, San Mateo, CA, USA). We report GJIC as a fraction of the control. Based on previous results (Upham et al. 1996, 1998), 1-methylanthracene as well as PFOA were used as positive controls of inhibition of GJIC, whereas acetonitrile at vehicle concentrations was used as a negative control. The vehicles used for the *in vitro* assays, acetonitrile and PBS, had no effect on GJIC. We performed all experiments at least in triplicate and report the results as means ± SD at the 95% confidence interval.

Western blot analysis. Cells were grown in 35-mm-diameter Corning tissue culture plates to the same confluency as the SL/DT assay. The cells were depleted of serum 5 hr before addition of PFFAs to synchronize the cells into G_0 to minimize background ERK levels. This does not alter the effect on GJIC in the F344 WB cells, as previously determined (Rummel et al. 1999). The proteins were extracted with 20% sodium dodecyl sulfate (SDS) solution containing 1 mM phenylmethylsulfonyl fluoride, 100 μM Na_3VO_4, 100 nM aprotinin, 1.0 μM leupeptin, 1.0 μM antipain, and 5.0 mM NaF. The protein content was determined with the Bio-Rad DC assay kit. The proteins were separated on 12.5% SDS–polyacrylamide gel electrophoresis according to the method of Laemmli

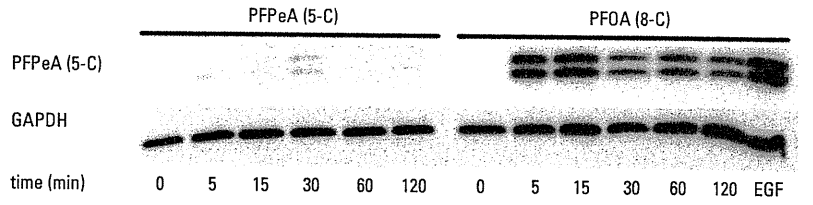

Figure 3. Activation of ERK-MAPK by PFOA, but not by PFPeA, in F344 WB rat liver epithelial cells determined by Western blots: Top panel probed with a phosphorylated ERK specific antibody and the bottom panel probed with a GAPDH specific antibody. The concentrations of PFPeA and PFOA were 100 μM. The concentration and time of incubation for epidermal growth factor (EGF) was 20.0 ng/mL and 15 min.

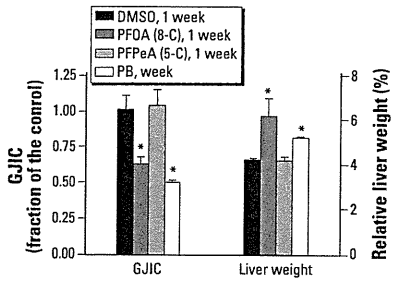

Figure 2. The long-term effects (1 week) of PB, PFOA, and PFPeA on GJIC and RLW (mean + SD). Abbreviations: 5-C, five carbon; 8-C, eight carbon. A one-way ANOVA was done for the GJIC data and a Kruskal-Wallis one-way ANOVA was done for the RLW data because these data failed the normality test.

*$p < 0.05$ compared with vehicle (DMSO); significant effects determined by ANOVA or Kruskal-Wallis ANOVA for each group was followed with a Dunnett's post hoc test at $p < 0.05$.

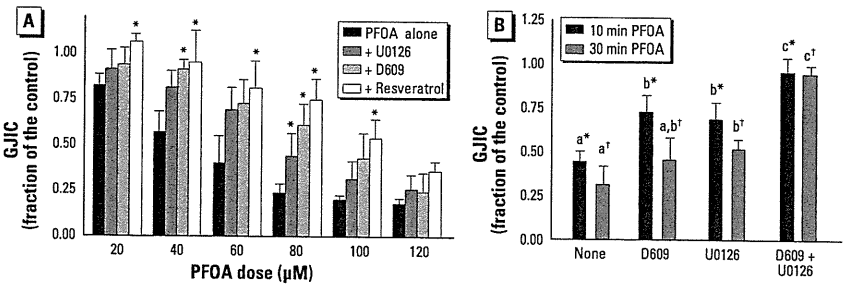

Figure 4. (*A*) Prevention of PFOA-induced inhibition of GJIC by inhibitors of MEK and PC-PLC and resveratrol at various doses of PFOA (mean + SD). The concentrations and times of preincubation of U0126, D609, and resveratrol were 20 μM/30 min, 50 μM/20 min, and 100 μM/15 min, respectively. A one-way ANOVA was done for each dose group. *Significant at $p < 0.05$ using the Dunnett's post hoc test that compared each inhibitor treatment with that of PFOA alone. (*B*) The interactive effect of MEK and PC-PLC inhibitors on reversing PFOA-induced inhibition of GJIC at 10 and 30 min (mean + SD). The concentrations and times of preincubation of U0126 and D609 were 20 μM/30 min and 50 μM/20 min, respectively. A one-way ANOVA indicated significance at $p < 0.05$ for each time group. The Tukey pairwise-comparison post hoc test was used to determine statistical differences, as indicated by different letters, between the inhibitor treatments for each time group. The lettered asterisks represent the 10-min group and lettered daggers represent the 30-min group.

(1970). Fifteen micrograms protein was loaded onto the gels and electrophoretically transferred from the gel to polyvinyl difluoride membranes (Millipore Corp., Bedford, MA, USA). Phosphorylated ERK 1 and ERK 2 were detected with a 1:2,000 dilution of anti-phospho-ERK polyclonal antibodies, and GAPDH was detected with a 1:10,000 dilution of anti-GAPDH polyclonal antibodies, that were incubated sequentially with the membranes, each for 2 hr. The protein–primary antibody complex was probed with a 1:1,000 dilution of horseradish peroxidase–conjugated anti-rabbit or anti-mouse antibodies (Amersham Life Science Products, Arlington Heights, IL, USA) for 1 hr. The ERK and GAPDH protein bands were detected using the Super Signal chemiluminescence detection kit (Pierce Corp., Arlington Heights, IL, USA), enhanced chemiluminescence (ECL) detection kit, and ECL Hyperfilm–MP (Amersham Life Science Products, Denver, CO, USA).

Statistics. For the *in vivo* studies, the value of each group was expressed as the mean ± SD of data derived from four rats. The *in vitro* assays were done in at least triplicate and expressed as a fraction of the control. The significance of differences in all results was evaluated with either a one-way analysis of variance (ANOVA) or, if the data set failed the normality test, a Kruskal-Wallis one-way ANOVA on ranked means. Normality assumption testing was done with the Kolmogorov-Smirnov test and equal variance assumption testing with the Levene median test. If ANOVA or Kruskal-Wallis ANOVA rejected the null hypothesis, then the results that were compared with a designated control used Dunnett's multiple-comparison post hoc tests or Tukey's post hoc test for pairwise multiple comparisons.

Results

In vivo *results.* The *in vivo* results of PFOA and PFPeA were compared with PB, a known liver tumor promoter. We used two different dosing schemes: an acute 24-hr exposure via i.p. administration and a longer-term (1 week) dietary exposure. An ANOVA indicated that PFOA, PFPeA, and PB had no statistically significant effect on body weights of the rats (data not shown). Liver injury was assessed using the biomarkers sALT, sAST, sALP, and the results for both dosing schemes are presented in Table 1. At day 7, there were no significant differences between the rats treated with PFOA, PFPeA, and PB for all three of the selected liver enzymes, indicating no long-term liver injury. After 1 day, we found a small, biologically insignificant, but statistically significant increase in sAST, with the data exhibiting high variability.

To assess the *in vivo* effects of these compounds on GJIC in the liver tissue, we used an IL/DT technique. Figure 1A shows the incorporation of the fluorescent dye into the liver cells and subsequent distribution of the fluorescent dye through the gap junctions of the tissue. RhD, which is a large-molecular-weight dye that does not traverse gap junctions, is color-coded red. LY, which does travel through gap junction channels, is color-coded from yellow for high intensity to green for lower intensity. We measured and averaged the distances traveled by the gap-junction–permeable dye and show them in Figure 1B (acute exposure) and Figure 2 (long-term exposure). PFOA and PB but not PFPeA inhibited *in vivo* GJIC in the liver tissues of rats treated either acutely or chronically. Significant inhibition of GJIC by PFOA was observed after 1 hr, and continued to inhibit GJIC until 24 hr in the acutely treated rats. Significant inhibition of GJIC did not begin until after 12 hr of treatment with PB in this group of rats.

In the acute dose regimen (Figure 1C), a significant increase in the relative weight of livers from rats treated with PFOA was observed at 24 hr. Similarly, rats chronically exposed to PFOA and PB for 1 week had significant increases in relative liver weight (RLW; Figure 2). The livers of animals treated either acutely or chronically with PFPeA did not significantly increase in relative weights compared with rats fed the vehicle (Figures 1C, 2).

In vitro *results.* Considering that the *in vitro* results of PFOA and PFPeA effects on gap junctions correlated with their effects on gap junctions *in vivo*, we did further *in vitro* analyses of PFOA to determine underlying mechanisms involved in the dysregulation of GJIC. PFOA, which inhibits GJIC, also activated ERK as determined by Western blot analysis of the phosphorylated, activated form of ERK (Figure 3). In contrast, the non-GJIC inhibitory PFPeA did not activate ERK (Figure 3). Activation of ERK was within 5 min in cells treated with PFOA, which correlates with the time of inhibition of GJIC, indicating a potential link. Preincubation of the cells with an MEK inhibitor, U0126, partially but significantly prevented the inhibition of GJIC by PFOA (Figure 4A). Preincubation of the cells with the PC-PLC inhibitor D609 also partially but significantly prevented the inhibition of GJIC by PFOA (Figure 4A). The significant contribution of PC-PLC and MEK in PFOA-induced inhibition of GJIC diminished after the maximum inhibitory dose of 80 μM to a nonsignificant involvement at the higher dose of 120 μM (Figure 4A), indicating further that mechanisms other than MEK and PC-PLC are also involved.

Gap junctions are known to be redox sensitive, so we conducted several experiments with various antioxidants. Resveratrol significantly reversed the inhibitory effect on GJIC and was possibly inhibiting both MEK and PC-PLC (Figure 4A). Additional experiments were performed to look at the combinatorial effect of pretreating cells with both D609 and U0126. The combination of both of these inhibitors of signal transduction enzymes resulted in the prevention of GJIC inhibition by PFOA, and the combinatorial effect was significantly greater than cells treated with either inhibitor alone as determined by a Tukey post hoc multiple-comparison test (Figure 4B). These results collectively indicate that PFOA-induced regulation of GJIC is a function of both of these signaling enzymes.

Further experiments were performed with DTT, Nac, and Asc-2-P (Figure 5). DTT

Table 1. The effect of PFOA, PFPeA, and PB on the levels of various biomarkers of liver injury in F344 rats.

	Enzyme activity (mU/mL)			
Exposure, time, enzyme	DMSO (vehicle)	PFOA	PFPeA	PB
Acute (24 hr)				
sALT	51.5 ± 3.2	138.6 ± 126.4	56.3 ± 13.2	54.5 ± 4.1
sAST	98.8 ± 8.8	232 ± 169.8*	113.0 ± 17.6	100.6 ± 15.1
sALP	1672.8 ± 90.0	1521.8 ± 220.2	1495.0 ± 233.8	1561.0 ± 115.2
Longer-term (1 week)				
sALT	39.3 ± 2.0	41.2 ± 1.9	39.8 ± 3.0	39.7 ± 2.6
sAST	71.2 ± 10.0	70.4 ± 4.3	73.9 ± 10.7	76.1 ± 9.4
sALP	1488.8 ± 62.9	1394.5 ± 59.4	1449.5 ± 36.6	1349.3 ± 53.0

To determine significant effects, we performed a one-way ANOVA for sALP (1 day), sALP (1 week), and sALT (1 week) and a Kruskal-Wallis one-way ANOVA on ranks for sAST (1 day), sAST (1 week), and sALT (1 day). Any significant effects determined by ANOVA were followed by a Dunnett's post hoc test, with DMSO designated as the control.
*$p < 0.05$.

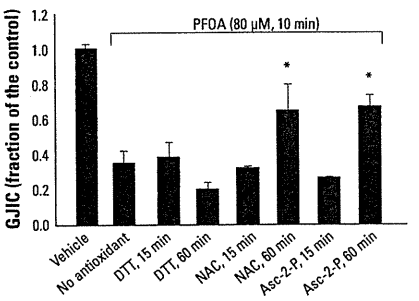

Figure 5. Prevention of PFOA-induced inhibition of GJIC by various antioxidants (mean + SD). The concentrations of PFOA, DTT, Nac, and Asc-2-P were 80 μM, 10 mM, 100 μM, and 100 μM, respectively.
*$p < 0.05$ by ANOVA and Dunnett's post hoc test comparing each antioxidant treatment with that of PFOA alone (no antioxidant).

and Nac in the absence of PFOA had no statistically (ANOVA) significant effect on GJIC at both 15 and 60 min (data not shown). Asc-2-P had a small, < 10% effect (ANOVA, Tukey) on GJIC in the absence of PFOA at 15 min but not 60 min (data not shown). Asc-2-P and Nac both prevented the inhibition of GJIC by PFOA within a 60-min preincubation time, but not DTT, implicating redox-sensitive proteins that probably do not involve thiol oxidations. Preincubation of Asc-2-P and Nac for 15 min did not reverse the effect of PFOA on GJIC. The oxidative nature of PFOA was not cytotoxic, as indicated after 2 days of growing cells after the log-phase of growth with 80 μM PFOA, resulting in no visual abnormalities in the morphology of the cells and complete restoration of GJIC after the cells were transferred to fresh medium for 5 hr containing no PFOA (Figure 6).

Discussion

Understanding the biological effects of the environmentally prevalent PFFAs on cell signaling pathways relevant to the epigenetic, nongenotoxic phase of cancer is important. In particular, GJIC offers a very central signaling system to assess risk (Trosko and Upham 2005). Although the transient closure of gap junction channels during proliferation is a normal response to mitogens, the chronic inhibition of GJIC by toxicants and toxins or by cytokines released during compensatory hyperplasia could lead to pathologic states (Trosko and Upham 2005; Upham and Trosko 2006). Thus, we conducted two dosing schemes, one a short term of 24 hr following an i.p. injection of PFOA, PFPeA, or PB, and another a longer-term study where the rats were dosed with these compounds through their daily feedings for 1 week. We previously demonstrated that inhibition of GJIC using *in vitro* model systems by perfluoroalkyl carboxylates and sulfonates depended on the chain length, where PFFAs with 7–10 carbons inhibited GJIC, and PFFAs with 2–6 carbons did not (Hu et al. 2002; Upham et al. 1998). To determine if chain length of PFFAs would exhibit similar effects on GJIC in a living organism, we treated F344 rats with PFOA, an eight-carbon PFFA, and PFPeA, a five-carbon PFFA, and determined GJIC in the liver tissue using an *ex vivo* IL/DT assay.

The liver is the primary target of PFOA (Kudo and Kawashima 2003), which is known to induce hepatocellular tumors in rodent model systems (Abdellatif et al. 1991; Kennedy et al. 2004). Similar to our *in vitro* results (Hu et al. 2002; Upham et al. 1998), PFOA decreased GJIC activity in the liver compared with the rats treated with the vehicle (control) for both the acute and long-term dosing schemes. In contrast, PFPeA-treated rats did not have altered GJIC in the livers compared with the control rats for both dosing schemes, which is also consistent with our *in vitro* observations. Another possible reason for the lack of an *in vivo* response by PFPeA could be a consequence of a greater elimination rate that is typical of PFFAs with shorter chain lengths (Chang et al. 2008; Ohmori et al. 2003). Although we did not measure the elimination rates of PFPeA in our experiments, the half-life of perfluorobutyrate is 9.2 hr (oral) and 6.4 hr (intravenous) in Sprague-Dawley rats (Chang et al. 2008). These half-lives are similar to that of PB in Sprague-Dawley rats, which is 8–9 hr. Considering that PB inhibited GJIC and induced hepatomegaly in the livers of the rats used in our experiments, and PFPeA did not inhibit GJIC using an *in vitro* assay system, we would expect that the noninhibitory effects of PFPeA on GJIC *in vivo* would not result from its increased rate of elimination. Further experiments are needed to confirm such a conclusion.

We previously published data that indicated the treatment of Sprague-Dawley rats with PFOS resulted in a decrease in GJIC activity in the liver tissue; thus, PFOA and PFOS have similar activities (Hu et al. 2002). The following are additional reports demonstrating that tumor promoters, known to inhibit GJIC *in vitro*, also inhibited GJIC *in vivo*: pentachlorophenol (Sai et al. 2000), 2-acetylaminofluorene (Krutovskikh et al. 1991), PB (Kolaja et al. 2000; Krutovskikh 1995), polychlorinated biphenyls (Kolaja et al. 2000; Krutovskikh 1995), pregnenolone-16α-carbonitrile (Kolaja et al. 2000), cadmium (Jeong et al. 2000), clofibrate, and DDT (Krutovskikh 1995). Another interesting report on the *in vivo* effects of chemicals on GJIC is the treatment of rats with the antioxidants lycopene and alpha and beta carotene. High doses of these antioxidants resulted in a decrease in GJIC activity, whereas rats exposed to low doses exhibited an increase in GJIC (Krutovskikh et al. 1997). Although *in vivo* assessment of intercellular communication has been limited in both the number of studies and choice of organ, namely, the liver, these results, including those presented in this report, nevertheless suggest that the *in vitro* rat liver epithelial cell assay system is a good predictor of the *in vivo* effects of chemicals on gap junctions in the liver tissues of rodents.

PFOA and PB induced hepatomegaly, whereas PFPeA had no effect. These results are similar to those previously published indicating that PFOA, but not perfluorobutyrate, affected RLWs in F344 rats (Takagi et al. 1991). Although not causally linked, hepatomegaly has been correlated with the promotion of liver tumors by many peroxisome proliferator-activated receptor α agonists, including PFOA (Takagi et al. 1992). The null effect of PFPeA on GJIC and hepatomegaly suggest that PFPeA would not be a tumor promoter; however, two-stage (initiation and promotion) carcinogenesis studies would be needed to confirm this conclusion. Tissue necrosis is known to induce compensatory hyperplasia that leads to increased liver weights, but this is unlikely the cause of hepatomegaly in the PFOA- and PB-treated rats, considering that no visual damage of the liver was seen in the histologic sections (data not shown) and there was no increase in serum enzymes.

Tissue homeostasis in multicellular organisms depends on functional GJIC, and the disruption of intercellular communication has been linked to many diseases (Trosko and Upham 2005). PFOA clearly interrupted GJIC in the liver tissues of rats, but further experiments would need to be done in other species. PFOS also inhibited GJIC in rat liver tissue as well as *in vitro* systems that included dolphin kidney cells (Hu et al. 2002). Thus, the potential for cross-species effects of PFOA on GJIC implicates a health risk to multicellular organisms. Future experiments, particularly with human cell lines, will aid in determining differences in the sensitivity of various organisms to the effects of PFOS and PFOA on GJIC and allow for more accurate assessment of risks these compounds pose to humans and wildlife.

Considering that *in vitro* analyses of PFFA, using rat liver epithelial cells, accurately predicted the *in vivo* effects on GJIC for various PFFAs, we did further *in vitro* analyses of PFPeA- and PFOA-treated rat liver epithelial cells to determine potential signaling mechanisms involved in PFOA-induced regulation of GJIC. Connexin 43 (Cx43) is a

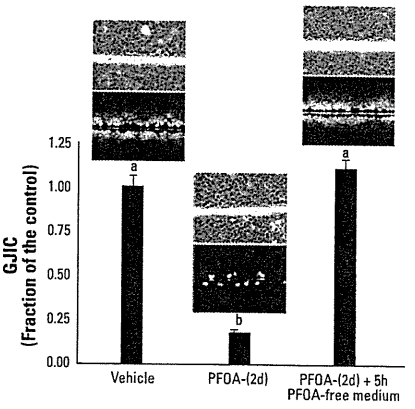

Figure 6. The effects of an extended incubation of cells with PFOA (80 μM, 2 days) and transfer of cells to PFOA-free medium (5 hr) on cell morphology and GJIC (mean + SD). Each phase-contrast and fluorescent photomicrograph represents one of the three replicates of each treatment group (magnification, 200×). Different letters indicate significance at $p < 0.05$ using ANOVA and Tukey post hoc test with a pairwise comparison.

phosphoprotein, and the phosphorylation of the carboxy terminus by protein kinases, such as protein kinase C (PKC), Src, and MAPKs, in the regulation of GJIC has been well documented (Solan and Lampe 2005). Although phosphorylation of gap junctions is known to regulate the function, assembly, internalization, and degradation of this protein complex, the alteration of connexin phosphorylation by protein kinases, such as MAPKs, does not necessarily dysregulate gap junction function (Hossain et al. 1999), nor does the activation of protein kinases (i.e., MAPK) alter the phosphorylation status of connexins (Upham et al. 2008).

This was also true for PFOA, which clearly activated ERK-MAPK (Figure 3) but did not induce a change in the phosphorylation pattern of Cx43 as previously determined by Western blot analysis (Upham et al. 1998). Whether or not gap junctions are phosphorylated, several compounds (i.e., growth factors, lindane, lysophosphatidic acid, 12-*O*-tetradecanoylphorbol-13-acetate, and cannabinoids) are known to inhibit GJIC through a MEK-dependent pathway (Komatsu et al. 2006; Mograbi et al. 2003; Rivedal and Opsahl 2001; Upham et al. 2003). Although many compounds activate MAPKs, such as p38 and ERK, the mechanism of inhibiting GJIC by many of these compounds is independent from these MAPKs (Machala et al. 2003; Upham et al. 2008).

Our results indicated that PFOA activated ERK in F344 WB rat liver epithelial cells within 5 min, and this time period is within the interval required for the inhibition of GJIC by PFOA in this cell line. PFPeA, which does not inhibit GJIC in this cell line (Upham et al. 1998), also did not activate ERK. Preincubation of these cells with an MEK inhibitor, U0126, partially prevented PFOA from inhibiting GJIC, indicating that PFOA-induced modulation of GJIC was not solely dependent on the ERK pathway.

Recently, PC-PLC has been implicated in the dysregulation of GJIC in response to toxicants that regulate GJIC through an MEK-independent mechanism (Machala et al. 2003; Upham et al. 2008). Preincubation of F344 WB cells with the PC-PLC inhibitor D609 also partially prevented PFOA from inhibiting GJIC. These results suggest that PFOA is regulating GJIC through multiple cellular mechanisms. This becomes more apparent as the dose of PFOA is increased resulting in the inhibition of GJIC at a high dose of 120 μM that depended on neither PC-PLC nor MEK. However, maximum inhibition of GJIC by PFOA, which was around 80 μM, was very dependent on the activity of both MEK and PC-PLC. This was further apparent from the experiment where cells were pretreated with a combination of both D609 and U0126, resulting in almost complete recovery of GJIC. The activation of ERK and PC-PLC will not only control gap junction function but is known to alter gene expression, leading to various pathologies, including cancer. The function of PC-PLC in tumorigenesis has not been extensively studied, yet there are significant reports indicating that PC-PLC does play a very significant role in cancer (Cheng et al. 1997). The ERK pathway has been extensively characterized and is the most understood of the MAPK pathways (Denhardt 1996) and is a key pathway of carcinogenesis (Roberts and Der 2007).

PFOA, but not perfluorobutyrate, is known to induce oxidative stress in the livers of rats, as indicated by 8-hydroxydeoxyguanosine formation (Takagi et al. 1991), and redox mechanisms are known to commonly play a role in gap junction function (Upham and Trosko 2009). These oxidative signaling effects could be site-directed redox regulations of specific regulatory proteins or from general oxidative effects (Upham and Trosko 2008). Recently, we reported that the antioxidant resveratrol prevented inhibition of GJIC by dicumylperoxide but not by benzoylperoxide (Upham et al. 2007). Dicumylperoxide, but not benzoylperoxide, inhibits GJIC through a PC-PLC–dependent mechanism (Upham et al. 2007). Similar to dicumylperoxide, we showed that resveratrol prevented inhibition of GJIC by PFOA to a greater level than either D609 or U0126 alone, but similar to the level of GJIC recovery seen when cells were pretreated with both D609 and U0126. These results indicate the possibility that PFOA dysregulates GJIC through both MEK and PC-PLC and that protection of GJIC by resveratrol is potentially through oxidative signaling events controlling both MEK and PC-PLC. Beyond the implication of redox mechanisms of the resveratrol experiment, this antioxidant is regularly consumed by humans and is found in high concentrations in red wine and peanut products (Sobolev and Cole 1999; Wang et al. 2002), and thus may have some relevance to the health of humans that may be exposed to environmental toxicants, such as PFOA. Chemopreventive effects of resveratrol are known to inhibit initiation, promotion, and progression of tumors (Signorelli and Ghidoni 2005). Thus, resveratrol could potentially contribute to a protective effect in humans exposed to PFOA by significantly blocking PFOA from inhibiting GJIC.

The addition of Asc-2-P or Nac partially reversed the inhibitory effects of PFOA on GJIC, similar to that of resveratrol. In contrast, DTT did not prevent PFOA from inhibiting GJIC, indicating that the oxidative events controlling PC-PLC and Mek are not thiol based. The exposure of F344 WB cells to PFOA for 2 days showed no adverse effects on cell morphology, and they communicated normally after PFOA was removed from the medium (Figure 6), which implicates that the PFOA-induced oxidative events are not killing the cells. These results suggest that general oxidative processes are involved in PFOA-induced inhibition of GJIC and that health benefits could potentially be attained by the consumption of many antioxidant rich foods, particularly in individuals deficient in antioxidants. Moreover, the reversible properties of PFOA-induced inhibition of GJIC are consistent with the known reversible nature of tumor promoters in two-stage carcinogenesis model systems (Trosko and Upham 2005). These results also indicate that reversing the effect of PFOA on GJIC after a simple washing of the treated cells with PBS demonstrates that PFOA is not covalently or tightly bound to the cell. The effect of PFOA on GJIC was probably not a consequence of directly interacting with the gap junction proteins because the inhibition of MAPK and PC-PLC both prevented the GJIC effect. Possibly PFOA interacted with these two proteins or interacted with a signaling protein or receptor even further upstream.

In conclusion, the *in vitro* assay system used to assess the effects of PFOA and PFPeA on GJIC predicted the *in vivo* results of GJIC from rats treated with these compounds. GJIC plays a vital role in maintaining tissue homeostasis, and disruption of gap junction function can lead to diseased states such as tumorigenesis. These results are similar to other tumor-promoting compounds tested in both an *in vitro* and *in vivo* assay system. Although there are several mechanisms by which environmental compounds might promote an initiated cell, such as through peroxisome proliferator activated receptors or protein kinase C, the disruption of normal intercellular communication is an essential event of multiple tumorigenic mechanisms (Trosko and Upham 2005) and serves as a central biomarker to assess the epigenetic toxicity of contaminants (Rosenkranz et al. 1997; Trosko and Upham 2005), as well as to assess the potential antitumorigenic health benefits of nutrition based food products (Trosko and Upham 2005).

References

Abdellatif AG, Preat V, Taper HS, Roberfroid M. 1991. The modulation of rat liver carcinogenesis by perfluorooctanoic acid, a peroxisome proliferator. Toxicol Appl Pharmacol 111(3):530–537.

Borek C, Sachs L. 1966. The difference in contact inhibition of cell replication between normal cells and cells transformed by different carcinogens. Proc Natl Acad Sci USA 56(1705):1705–1711.

Calafat AM, Wong LY, Kuklenyik Z, Reidy JA, Needham LL. 2007. Polyfluoroalkyl chemicals in the U.S. population: data from the National Health and Nutrition Examination Survey (NHANES) 2003–2004 and comparisons with NHANES 1999–2000. Environ Health Perspect 115:1596–1602.

Cattley RC, Miller RT, Corton JC. 1995. Peroxisome proliferators: potential role of altered hepatocyte growth and

differentiation in tumor development. Prog Clin Biol Res 391:295–303.

Chang SC, Das K, Ehresman DJ, Ellefson ME, Gorman GS, Hart JA, et al. 2008. Comparative pharmacokinetics of perfluorobutyrate in rats, mice, monkeys, and humans and relevance to human exposure via drinking water. Toxicol Sci 104(1):40–53.

Cheng J, Weber JD, Baldassare JJ, Raben DM. 1997. Ablation of Go alpha-subunit results in a transformed phenotype and constitutively active phosphatidylcholine-specific phospholipase C. J Biol Chem 272(28):17312–17319.

Coleman WB, Wennerberg AE, Smith GJ, Grisham JW. 1993. Regulation of the differentiation of diploid and some aneuploid rat liver epithelial (stemlike) cells by the hepatic microenvironment. Am J Pathol 142(5):1373–1382.

Denhardt DT. 1996. Signal-transducing protein phosphorylation cascades mediated by Ras/Rho proteins in the mammalian cell: the potential for multiplex signalling. Biochem J 318(pt 3):729–747.

DeWitt JC, Copeland CB, Strynar MJ, Luebke RW. 2008. Perfluorooctanoic acid–induced immunomodulation in adult C57BL/6J or C57BL/6N female mice. Environ Health Perspect 116:645–650.

Hekster FM. 2003. Environmental and toxicity effects of perfluoroalkylated substances. Rev Environ Contam Toxicol 79:99–121.

Hossain MZ, Jagdale AB, Ao P, Boynton AL. 1999. Mitogen-activated protein kinase and phosphorylation of connexin43 are not sufficient for the disruption of gap junctional communication by platelet-derived growth factor and tetradecanoylphorbol acetate. J Cell Physiol 179(1):87–96.

Hu W, Jones PD, Upham BL, Trosko JE, Lau C, Giesy JP. 2002. Inhibition of gap junctional intercellular communication by perfluorinated compounds in rat liver and dolphin kidney epithelial cell lines in vitro and Sprague-Dawley rats in vivo. Toxicol Sci 68(2):429–436.

Jeong SH, Habeebu SSM, Klaassen CD. 2000. Cadmium decreases gap junctional intercellular communication in mouse liver. Toxicol Sci 57(1):156–166.

Kannan K. 2001. Accumulation of perfluorooctane sulfonate in marine mammals. Environ Sci Technol 35(8):1593–1598.

Kennedy GL, Butenhoff JL, Olsen GW, O'Connor JC, Seacat AM, Perkins RG, et al. 2004. The toxicology of perfluorooctanoate. Crit Rev Toxicol 34(4):351–384.

Key BD, Howell RD, Criddle CS. 1997. Fluorinated organics in the biosphere. Environ Sci Technol 31:2445–2454.

Klaunig JE, Babich MA, Baetcke KP, Cook JC, Corton JC, David RM, et al. 2003. PPARalpha agonist-induced rodent tumors: modes of action and human relevance. Crit Rev Toxicol 33(6):655–780.

Kolaja KL, Engelken DT, Klaassen CD. 2000. Inhibition of gap-junctional-intercellular communication in intact rat liver by nongenotoxic hepatocarcinogens. Toxicology 146(1):15–22.

Komatsu J, Yamano S, Kuwahara A, Tokumura A, Irahara M. 2006. The signaling pathways linking to lysophosphatidic acid-promoted meiotic maturation in mice. Life Sci 79(5):506–511.

Krutovskikh VA. 1995. Inhibition of rat liver gap junction intercellular communication by tumor-promoting agents in vivo. Association with aberrant localization of connexin proteins. Lab Invest 72(5):571–577.

Krutovskikh V, Asamoto M, Takasuka N, Murakoshi M, Nishino H, Tsuda H. 1997. Differential dose-dependent effects of alpha-, beta-carotenes and lycopene on gap-junctional intercellular communication in rat liver in vivo. Jpn J Cancer Res 88(12):1121–1124.

Krutovskikh VA, Oyamada M, Yamasaki H. 1991. Sequential changes of gap-junctional intercellular communications during multistage rat liver carcinogenesis: direct measurement of communication in vivo. Carcinogenesis 12(9):1701–1706.

Kudo N, Kawashima Y. 2003. Toxicity and toxicokinetics of perfluorooctanoic acid in humans and animals. J Toxicol Sci 28(2):49–57.

Laemmli UK. 1970. Cleavage of structural proteins during the assembly of the head of bacteriophage T4. Nature 227:680–685.

Machala M, Blaha L, Vondracek J, Trosko JE, Scott J, Upham BL. 2003. Inhibition of gap junctional intercellular communication by noncoplanar polychlorinated biphenyls: inhibitory potencies and screening for potential mode(s) of action. Toxicol Sci 76(1):102–111.

Mograbi B, Corcelle E, Defamie N, Samson M, Nebout M, Segretain D, et al. 2003. Aberrant connexin 43 endocytosis by the carcinogen lindane involves activation of the ERK/mitogen-activated protein kinase pathway. Carcinogenesis 24(8):1415–1423.

Ohmori K, Kudo N, Katayama K, Kawashima Y. 2003. Comparison of the toxicokinetics between perfluorocarboxylic acids with different carbon chain length. Toxicology 184(2–3):135–140.

Potter VR. 1978. Phenotypic diversity in experimental hepatomas: the concept of partially blocked ontogeny. Br J Cancer 38(1):1–23.

Rivedal E, Opsahl H. 2001. Role of PKC and MAP kinase in EGF- and TPA-induced connexin43 phosphorylation and inhibition of gap junction intercellular communication in rat liver epithelial cells. Carcinogenesis 22(9):1543–1550.

Roberts PJ, Der CJ. 2007. Targeting the Raf-MEK-ERK mitogen-activated protein kinase cascade for the treatment of cancer. Oncogene 26(22):3291–3310.

Rosenkranz M, Rosenkranz HS, Klopman G. 1997. Intercellular communication, tumor promotion and non-genotoxic carcinogenesis: relationships based upon structural considerations. Mutat Res 381(2):171–188.

Rummel AM, Trosko JE, Wilson MR, Upham BL. 1999. Polycyclic aromatic hydrocarbons with bay-like regions inhibited gap junctional intercellular communication and stimulated MAPK activity. Toxicol Sci 49(2):232–240.

Sai K, Kanno J, Hasegawa R, Trosko JE, Inoue T. 2000. Prevention of the down-regulation of gap junctional intercellular communication by green tea in the liver of mice fed pentachlorophenol. Carcinogenesis 21(9):1671–1676.

Signorelli P, Ghidoni R. 2005. Resveratrol as an anticancer nutrient: molecular basis, open questions and promises. J Nutr Biochem 16(8):449–466.

Skutlarek D, Exner M, Farber H. 2006. Perfluorinated surfactants in surface and drinking waters. Environ Sci Pollut Res Int 13(5):299–307.

Sobolev VS, Cole RJ. 1999. trans-resveratrol content in commercial peanuts and peanut products. J Agric Food Chem 47(4):1435–1439.

Solan JL, Lampe PD. 2005. Connexin phosphorylation as a regulatory event linked to gap junction channel assembly. Biochim Biophys Acta 1711(2):154–163.

Takagi A, Sai K, Umemura T, Hasegawa R, Kurokawa Y. 1991. Short-term exposure to the peroxisome proliferators, perfluorooctanoic acid and perfluorodecanoic acid, causes significant increase of 8-hydroxydeoxyguanosine in liver DNA of rats. Cancer Lett 57(1):55–60.

Takagi A, Sai K, Umemura T, Hasegawa R, Kurokawa Y. 1992. Hepatomegaly is an early biomarker for hepatocarcinogenesis induced by peroxisome proliferators. J Environ Pathol Toxicol Oncol 11:145–149.

Tao L. 2006. Perfluorooctanesulfonate and related fluorochemicals in albatrosses, elephant seals, penguins, and polar skuas from the Southern Ocean. Environ Sci Technol 40(24):7642–7648.

Trosko JE, Ruch RJ. 1998. Cell-cell communication in carcinogenesis. Front Biosci 3:208–236.

Trosko JE, Ruch RJ. 2002. Gap junctions as targets for cancer chemoprevention and chemotherapy. Curr Drug Targets 3(6):465–482.

Trosko JE, Upham BL. 2005. The emperor wears no clothes in the field of carcinogen risk assessment: ignored concepts in cancer risk assessment. Mutagenesis 20(2):81–92.

Tsao MS, Smith JD, Nelson KG, Grisham JW. 1984. A diploid epithelial cell line from normal adult rat liver with phenotypic properties of "oval" cells. Exp Cell Res 154(1):38–52.

Upham BL, Blaha L, Babica P, Park JS, Sovadinova I, Pudrith C, et al. 2008. Tumor promoting properties of a cigarette smoke prevalent polycyclic aromatic hydrocarbon as indicated by the inhibition of gap junctional intercellular communication via phosphatidylcholine-specific phospholipase C. Cancer Sci 99(4):696–705.

Upham BL, Deocampo ND, Wurl B, Trosko JE. 1998. Inhibition of gap junctional intercellular communication by perfluorinated fatty acids is dependent on the chain length of the fluorinated tail. Int J Cancer 78(4):491–495.

Upham BL, Guzvic M, Scott J, Carbone JM, Blaha L, Coe C, et al. 2007. Inhibition of gap junctional intercellular communication and activation of mitogen-activated protein kinase by tumor-promoting organic peroxides and protection by resveratrol. Nutr Cancer 57(1):38–47.

Upham BL, Rummel AM, Carbone JM, Trosko JE, Ouyang Y, Crawford RB, et al. 2003. Cannabinoids inhibit gap junctional intercellular communication and activate ERK in a rat liver epithelial cell line. Int J Cancer 104(1):12–18.

Upham BL, Trosko JE. 2006. A paradigm shift in the understanding of oxidative stress and it's implications to exposure of low-level ionizing radiation. Acta Med Nagasaki 50:63–68.

Upham BL, Trosko JE. 2009. Oxidative-dependent integration of signal transduction with intercellular gap junctional communication in the control of gene expression. Antioxid Redox Signal 11(2):297–307.

Upham BL, Weis LM, Rummel AM, Masten SA, Trosko JE. 1996. The effects of anthracene and methylated anthracenes on gap junctional intercellular communication in rat liver epithelial cells. Fundam Appl Toxicol 34(2):260–264.

Van de Vijver KI. 2005. Tissue distribution of perfluorinated chemicals in harbor seals (*Phoca vitulina*) from the Dutch Wadden Sea. Environ Sci Technol 39(18):6978–6984.

Wang Y, Catana F, Yang Y, Roderick R, van Breemen RB. 2002. An LC-MS method for analyzing total resveratrol in grape juice, cranberry juice, and in wine. J Agric Food Chem 50(3):431–435.

feeding or satiation or to assess the ability of glucose to alter neuronal activity or the release of peptides (Levin et al., 2004; Parton et al., 2007). Such nonphysiological glucose levels provide little useful evidence for a physiological role of glucose in vitro or in vivo in the regulation of neuronal function or energy and glucose homeostasis. Thus, after more than 50 years, we are still in search of a direct link between neuronal glucose sensing and the physiological regulation of food intake and other facets of energy and glucose homeostasis. However, the Claret et al. (2007) and Parton et al. (2007) studies do point to important glucose-sensing-independent roles for both AMPK and the K_{ATP} channel in POMC neurons in the control of these physiological processes, which should be the focus of future studies in this field.

REFERENCES

Ashford, M.L.J., Boden, P.R., and Treherne, J.M. (1990). Pflugers Arch. *415*, 479–483.

Claret, M., Smith, M.A., Batterham, R.L., Selman, C., Choudhury, A.I., Fryer, L.G.D., Clements, M., Al-Qassab, H., Heffron, H., Xu, A.W., et al. (2007). J. Clin. Invest. *117*, 2325–2336.

de Vries, M.G., Arseneau, L.M., Lawson, M.E., and Beverly, J.L. (2003). Diabetes *52*, 2767–2773.

Escartin, C., Pierre, K., Colin, A., Brouillet, E., Delzescaux, T., Guillermier, M., Dhenain, M., Deglon, N., Hantraye, P., Pellerin, L., and Bonvento, G. (2007). J. Neurosci. *27*, 7094–7104.

Fioramonti, X., Contie, S., Song, Z., Routh, V.H., Lorsignol, A., and Penicaud, L. (2007). Diabetes *56*, 1219–1227.

Levin, B.E., Routh, V.H., Kang, L., Sanders, N.M., and Dunn-Meynell, A.A. (2004). Diabetes *53*, 2521–2528.

Mayer, J. (1953). N. Engl. J. Med. *249*, 13–16.

Minokoshi, Y., Alquier, T., Furukawa, N., Kim, Y.B., Lee, A., Xue, B., Mu, J., Foufelle, F., Ferre, P., Birnbaum, M.J., et al. (2004). Nature *428*, 569–574.

Mountjoy, P.D., Bailey, S.J., and Rutter, G.A. (2007). Diabetologia *50*, 168–177.

Oomura, Y., Kimura, K., Ooyama, H., Maeo, T., Iki, M., and Kuniyoshi, N. (1964). Science *143*, 484–485.

Parton, L.E., Ye, C.P., Coppari, R., Enriori, P.J., Choi, B., Zhang, C.Y., Xu, C., Vianna, C.R., Balthasar, N., Lee, C.E., et al. (2007). Nature *449*, 228–232.

Estrogen and Bone: Osteoclasts Take Center Stage

Deborah V. Novack[1,*]
[1]Department of Internal Medicine and Department of Pathology and Immunology, Division of Bone and Mineral Diseases, Washington University School of Medicine, St. Louis, MO 63110, USA
*Correspondence: novack@wustl.edu
DOI 10.1016/j.cmet.2007.09.007

Loss of estrogen at menopause causes osteoporosis in many women, but estrogen's relevant cellular target in this process has remained unclear. In a recent study in *Cell*, Kato and colleagues (Nakamura et al., 2007) selectively ablate estrogen receptor α in osteoclasts and demonstrate that estrogen directly induces osteoclast apoptosis.

Estrogen plays a central role in the control of bone strength, and its loss at menopause causes osteoporosis in millions of women. In healthy individuals, bone mass is maintained by the balanced activity of bone-forming osteoblasts and bone-resorbing osteoclasts. These two cell types, although derived from mesenchymal and hematopoietic precursors, respectively, affect each other's differentiation and activity. In addition, bone, particularly the trabecular component closely associated with bone marrow, is a rich microenvironment in which many cell types have the opportunity to influence osteoblast/osteoclast dynamics.

Osteoporosis, at the outset, is a disease of increased bone turnover in which the bone-resorbing activity of osteoclasts outpaces the bone-forming activity of osteoblasts, leading to loss of predominantly trabecular bone. Both of these cell types are reported to respond to estrogen. However, many studies suggest that bone's response to estrogen withdrawal is at least in part mediated by a network of inflammatory and osteoclastogenic cytokines including TNFα and IL-1, released by stromal/osteoblast lineage cells and T cells (Figure 1A) (Clowes et al., 2005). Thus, the critical estrogen target cell has been a matter of considerable debate.

Most estrogenic effects are mediated by the nuclear hormone receptor transcription factors estrogen receptor α and β (ERα and β); some actions are attributed to an unidentified membrane receptor that signals through JNK or ERK kinases. Mice lacking ERα, ERβ, or both do not show the expected low bone mass but have abnormally high levels of either testosterone or estradiol, leading to confounding effects on the androgen receptor (Sims et al., 2002). Further studies in which sex steroid levels were controlled by gonadectomy and

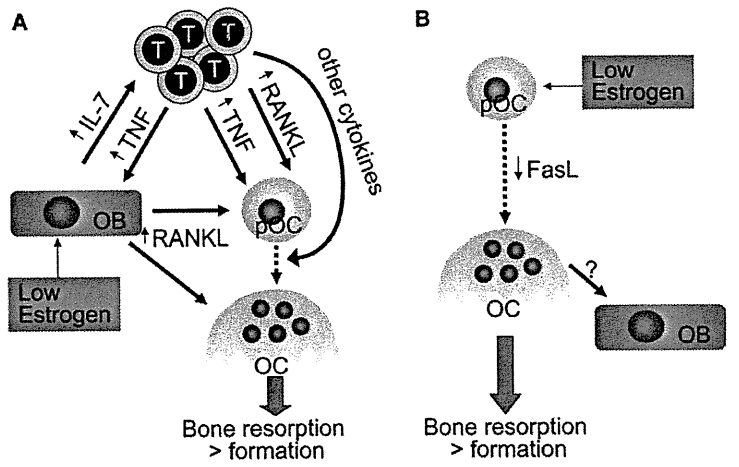

Figure 1. Models of Osteoclast Activation

(A) Hypothetical model of immune regulation of postmenopausal osteoporosis, in which osteoblast lineage cells (OBs) are the primary estrogen target. Decreased levels of estrogen lead to increased production of the cytokine IL-7 by OBs, promoting proliferation of T cells and their secretion of both TNF and RANKL. TNF stimulates OBs to increase their synthesis of RANKL, which leads to osteoclast (OC) differentiation and activation. TNF also acts directly on osteoclast progenitors (pOCs), synergizing with RANKL for OC differentiation. Additional pro-osteoclastogenic cytokines and growth factors are also expressed by T cells and other peripheral blood mononuclear cells.

(B) Model of direct estrogen action on osteoclasts, based on Nakamura et al. (2007). Estrogen, acting via ERα, causes upregulation of FasL by pOCs and/or OCs. Since these OC lineage cells also express Fas, increased FasL levels cause apoptosis, limiting the number and life span of OCs. In the absence of estrogen, FasL expression is lost, and OC life span is prolonged. Surviving OCs stimulate osteoblasts to form more bone (via poorly defined factors), but the resorptive effect is dominant. In both (A) and (B), the net effect of estrogen loss is increased by osteoclastic bone resorption that outpaces osteoblastic bone formation.

estrogen treatment suggest that ERα plays the dominant role in regulating bone mass in both males and females (Sims et al., 2003). However, the artificial manipulation of sex steroids and the global deletion of the receptors left open many questions about the direct impact of estrogen on bone cells.

In a recent issue of *Cell*, Kato and colleagues (Nakamura et al., 2007) employ an elegant approach to analyze the direct effect of estrogen on osteoclasts. Taking advantage of a previously described conditional *ERα* allele (Dupont et al., 2000), the authors inserted the Cre recombinase into the cathepsin K (*Ctsk*) locus, allowing them to specifically delete ERα during osteoclastogenesis. These $ER\alpha^{\Delta Oc/\Delta Oc}$ mice have normal levels of sex steroids, removing a major factor confounding previous approaches. Adult female, but not male, $ER\alpha^{\Delta Oc/\Delta Oc}$ mice displayed high bone turnover osteoporosis, with decreased trabecular bone mass, increased osteoclast numbers, and increased bone formation. These $ER\alpha^{\Delta Oc/\Delta Oc}$ mice, therefore, seem to mimic human postmenopausal osteoporosis to a greater extent than previous mouse models. The abrupt loss of estrogen following ovariectomy caused loss of trabecular bone and increased osteoclast numbers in wild-type mice, but not in $ER\alpha^{\Delta Oc/\Delta Oc}$ mice, despite apparently intact induction of TNFα and IL-1α. Additionally, although estrogen treatment following ovariectomy effectively reversed trabecular bone loss in controls, similar treatment of $ER\alpha^{\Delta Oc/\Delta Oc}$ mice did not increase bone mass. Thus, despite the presence of estrogen-responsive osteoblasts, T cells, and other potential targets, acute manipulation of estrogen levels has no effect on trabecular bone when osteoclasts are unable to respond directly to estrogen.

Several groups have reported direct induction of osteoclast apoptosis by estrogen in vitro, but whether this occurs in vivo was left unclear. Nakamura et al. (2007) find apoptotic, FasL-expressing osteoclasts in the bones of estrogen-treated ovariectomized wild-type mice. Osteoclasts lacking ERα do not upregulate FasL, either in vivo or in vitro, and do not undergo apoptosis following estrogen treatment. Fas, the death receptor required for an apoptotic response to FasL, is also expressed by osteoclasts but is not regulated by estrogen. Thus, estrogen-mediated upregulation of FasL appears to control osteoclast life span in an autocrine manner (Figure 1B). Although in most instances Fas and FasL are expressed in different cells, apoptosis of single T cells expressing both proteins has been described (Brunner et al., 1995). However, the mechanism by which Fas and FasL expressed by the same cell might interact remains unknown.

One puzzling finding is that, in the ovariectomized $ER\alpha^{\Delta Oc/\Delta Oc}$ mice, TNF levels are increased, but there is no effect on osteoclast numbers or bone mass. TNF is a potent osteoclastogenic factor that induces RANKL on osteoblast lineage cells and also acts directly on osteoclasts and their precursors. It is not clear why TNF and the RANKL it induces locally do not act on ERα-deficient osteoclast lineage cells to enhance bone resorption, since the response to these cytokines is independent of estrogen. Are the $ER\alpha^{\Delta Oc/\Delta Oc}$ mice already at the upper limit of their osteoclastogenic response prior to ovariectomy?

In isolation, the data derived from the osteoclast-specific deletion of ERα convincingly indicate that the osteoclast is the key estrogen target for the maintenance of bone mass. However, it is difficult to ignore myriad other studies in both mice and humans suggesting that the immune system and a host of inflammatory cytokines are activated upon estrogen withdrawal, with adverse effects on bone mass (Clowes et al., 2005). In many studies using genetically modified mice, removal of response to a single factor (such as TNF, IL-6, IL-7, or IL-11) has been found to block bone loss following ovariectomy. It is difficult to envision how each factor could

exert such a dominant effect when the normal physiological response involves upregulation of so many distinct factors. Most investigators have concluded that several cytokines have unique yet interconnected roles in the pathogenesis of osteoporosis. Similarly, although removal of ERα only from the osteoclast ablates the response to changes in estrogen, it is likely that deleting the receptor from other estrogen-responsive cells will reveal additional critical cellular targets for estrogen, generating a more complete picture of the complex process of postmenopausal bone loss.

REFERENCES

Brunner, T., Mogil, R.J., LaFace, D., Yoo, N.J., Mahboubi, A., Echeverri, F., Martin, S.J., Force, W.R., Lynch, D.H., Ware, C.F., et al. (1995). Nature *373*, 441–444.

Clowes, J.A., Riggs, B.L., and Khosla, S. (2005). Immunol. Rev. *208*, 207–227.

Dupont, S., Krust, A., Gansmuller, A., Dierich, A., Chambon, P., and Mark, M. (2000). Development *127*, 4277–4291.

Nakamura, T., Imai, Y., Matsumoto, T., Sato, S., Takeuchi, K., Igarashi, K., Harada, Y., Azuma, Y., Krust, A., Yamamoto, Y., et al. (2007). Cell *130*, 811–823.

Sims, N.A., Dupont, S., Krust, A., Clement-Lacroix, P., Minet, D., Resche-Rigon, M., Gaillard-Kelly, M., and Baron, R. (2002). Bone *30*, 18–25.

Sims, N.A., Clement-Lacroix, P., Minet, D., Fraslon-Vanhulle, C., Gaillard-Kelly, M., Resche-Rigon, M., and Baron, R. (2003). J. Clin. Invest. *111*, 1319–1327.

0026-895X/07/7205-1171–1180$20.00
MOLECULAR PHARMACOLOGY

Mol Pharmacol 72:1171–1180, 2007

Vol. 72, No. 5
38836/3268509
Printed in U.S.A.

Evaluation of Action Mechanisms of Toxic Chemicals Using JFCR39, a Panel of Human Cancer Cell Lines[S]

Noriyuki Nakatsu, Tomoki Nakamura, Kanami Yamazaki, Soutaro Sadahiro, Hiroyasu Makuuchi, Jun Kanno, and Takao Yamori

Division of Molecular Pharmacology, Cancer Chemotherapy Center, Japanese Foundation for Cancer Research, Koto-ku, Tokyo, Japan (N.N., T.N., K.Y., T.Y.); Division of Cellular and Molecular Toxicology, Biological Safety Research Center, National Institute of Health Sciences, Setagaya-ku, Tokyo, Japan (N.N., J.K.); and Second Department of Surgery, Tokai University School of Medicine, Boseidai, Isehara-City, Kanagawa, Japan (T.N., S.S., H.M.)

Received June 6, 2007; accepted August 16, 2007

ABSTRACT

We previously established a panel of human cancer cell lines, JFCR39, coupled to an anticancer drug activity database; this panel is comparable with the NCI60 panel developed by the National Cancer Institute. The JFCR39 system can be used to predict the molecular targets or evaluate the action mechanisms of the test compounds by comparing their cell growth inhibition profiles (i.e., fingerprints) with those of the standard anticancer drugs using the COMPARE program. In this study, we used this drug activity database-coupled JFCR39 system to evaluate the action mechanisms of various chemical compounds, including toxic chemicals, agricultural chemicals, drugs, and synthetic intermediates. Fingerprints of 130 chemicals were determined and stored in the database. Sixty-nine of 130 chemicals (~60%) satisfied our criteria for the further analysis and were classified by cluster analysis of the fingerprints of these chemicals and several standard anticancer drugs into the following three clusters: 1) anticancer drugs, 2) chemicals that shared similar action mechanisms (for example, ouabain and digoxin), and 3) chemicals whose action mechanisms were unknown. These results suggested that chemicals belonging to a cluster (i.e., a cluster of toxic chemicals, a cluster of anticancer drugs, etc.) shared similar action mechanism. In summary, the JFCR39 system can classify chemicals based on their fingerprints, even when their action mechanisms are unknown, and it is highly probable that the chemicals within a cluster share common action mechanisms.

Determining the action mechanism or identifying the molecular target of a chemical with pharmacological activity or adverse side effects is highly desirable. Although various test methods are currently available for determining the action mechanisms of chemicals, such as methods based on animal models, methods based on cellular models, bacterial mutagenicity test, the uterotropic assay (Kanno et al., 2002), Hershberger test (Hershberger et al., 1953), and the reporter assay for the nuclear receptor agonists, determination of the action mechanisms of pharmacologically active chemicals, including the toxic chemicals, is still a difficult and challenging task. Therefore, it is highly desirable to develop efficient test methods for evaluating toxicity of chemicals.

A number of screening methods are currently available for discovering new anticancer drugs. One very powerful and unique approach using multiple cancer cell lines was developed at NCI (Paull et al., 1989; Weinstein et al., 1992, 1997) and in our laboratory (Yamori et al., 1999; Dan et al., 2002, 2003; Yamori, 2003; Nakatsu et al., 2005; Akashi and Yamori, 2007; Akashi et al., 2007; Nakamura et al., 2007). This bioinformatics-based approach enables mechanism-oriented evaluation of anticancer drugs. For example, we can evaluate the cell toxicity in vitro by determining the 50% growth inhibition (GI50), total growth inhibition, and 50% lethal concentration across a panel of 39 human cancer cell lines (JFCR39). We can also predict the molecular targets or evaluate the action mechanisms of the test compounds by comparing the cell growth inhibition profiles (termed "fingerprints") across the panel for these compounds with those of

This work was supported in part by Grant-in-Aid 17390032 for Scientific Research (B) from Japan Society for the Promotion of Science (to T.Y.); Ministry of Health, Labor, and Welfare Grants-in-Aid H15-kagaku-002, H16-kagaku-003 (to T.Y. and J.K.); Grant-in-Aid 18015049 of the Priority Area "Cancer" from the Ministry of Education, Culture, Sports, Science and Technology of Japan (to T.Y.); and grant 05-13 from National Institute of Biomedical Innovation Japan (to T.Y.)

N. N. and T. N. equally contributed to this study.

Article, publication date, and citation information can be found at http://molpharm.aspetjournals.org.
doi:10.1124/mol.107.038836.

[S] The online version of this article (available at http://molpharm.aspetjournals.org) contains supplemental material.

ABBREVIATIONS: GI50, 50% growth inhibition concentration; GI50, 50% growth inhibition; SN-38, 7-ethyl-10-hydroxycamptothecin; SV-NN, snake venom from *N. nigricollis*; SV-NNK; snake venom from *N. naja kaouthia*.

TABLE 1
List of chemicals tested. Chemical names, abbreviations, and applications/targets/mechanisms of the test compounds are summarized.

JCI No	Name	Abbreviation	Application/Target/Mechanism
−691	Trioctyltin	TOT	Organotin
−690	Triphenyltin	TPT	Organotin
−689	Dibutyltin		Organotin
−688	AM-580		RARα
−687	TTNPB		RAR
−686	13-*cis* Retinoic acid	13-*cis*	RAR
−607	Methoprene		Agricultural chemical
−606	Methoprene acid		RXR
−605	5-aza-2′-deoxycytidine	5-AzaC	Methylation
−604	Carbaryl		Agricultural chemical
−603	Acephate		Agricultural chemical
−602	Sodium arsenite		Agricultural chemical
−601	Testosterone propionate	TP	Testosterone
−600	Ethynyl estradiol	EE	Estrogenic
−599	Thiram		Agricultural chemical
−598	Dimethylformamide	DMF	Solvent
−568	α-Bungarotoxin	αBuTX	Neurotoxin
−567	Snake venom from *Trimeresurus flavoviridis*	SV-TF	Snake venom
−566	Snake venom from *Crotalus atrox*	SV-CA	Snake venom
−565	Snake venom from *Agkistrodon halys blomhoffii*	SV-AHB	Snake venom
−564	Dexamethasone	DEX	Steroid
−563	3-Methylcholanthrene	3-MC	Teratogenicity/carcinogenicity
−562	*N*-Ethyl-*N*-nitrosourea	ENU	Teratogenicity/carcinogenicity
−561	Diethylnitrosamine	DEN	Teratogenicity/carcinogenicity
−560	All *trans*-retinoic acid	ATRA	RAR + RXR
−559	9-cis Retinoic acid	9-cis	RAR
−558	Levothyroxine	T4	Thyroid hormone
−557	3-Amino-1*H*-1,2,4-triazole	3AST	Agricultural chemical
−555	2-Vinylpyridine	2VP	Synthetic intermediate
−553	Phenobarbital	PB	Antiepileptic
−552	Acetaminophen	APAP	Analgetic
−551	Isoniazid		Phthisic
−549	4-Ethylnitrobenzene	4ENB	Synthetic intermediate
−548	1,2-Dichloro-3-nitrobenzene	1,2DC3NB	Pigment/synthetic intermediate
−546	*N*-Methylaniline	NMA	Synthetic intermediate
−545	2-Aminomethylpyridine	2AMP	Synthetic intermediate
−544	1*H*-1,2,4-Triazole		Synthetic intermediate
−543	1*H*-1,2,3-Triazole		Synthetic intermediate
−542	4-Amino-2,6-dichlorophenol	4A2,6DCP	Synthetic intermediate
−541	2,4-Dinitrophenol	2,4 DNP	Agricultural chemical
−513	Capsaicin		Food constituent
−485	2-Methoxyestradiol		Estrogenic
−466	Colcemid		Spindle inhibitor
−465	2,4-Dinitrochlorobenzene	2,4DCB	Pigment/mutagenesis
−464	Troglitazone		Diabetic
−463	Clofibrate		Antilipemic
−459	Bis(2-ethylhexyl)phthalate	DEHP	Plasticizer
−458	Thiourea		Agricultural chemical
−447	Cacodylic acid		Agricultural chemical
−446	Amitrole		Agricultural chemical
−445	4-Octylphenol	OP	Reproductive effector
−444	2,6-Dimethylaniline	2,6-Xylidene	Natural product
−443	1,2-Dibromo-3-chloropropane	DBCP	Agricultural chemical
−442	1,1-Dimethylhydrazine	1,1DMH	Reproductive effector
−441	Sulfanylamide		Agricultural chemical
−440	Streptozotocin		Agricultural chemical
−439	Spironolactone		Aldosterone antagonist
−438	*para*-Aminoazobenzene	pAAB	Pigment/mutagenicity/carcinogenicity
−437	*para*-Cresidine		Pigment/carcinogenicity
−436	Neostigmine bromide		Parasympathomimetics
−435	*para*-Dichlorobenzene	pDCB	Pigment/Agricultural chemical
−434	Phenytoin		Antiepileptic
−433	*ortho*-Toluidine	oToluidine	Pigment
−432	Imipramine		Antidepressant
−431	Cobalt chloride		Teratogenicity/mutagenicity
−428	Atrazine		Agricultural chemical
−427	Propylthiouracil		Teratogenicity/carcinogenicity
−426	Thalidomide (L + D)		Teratogenicity
−425	Carbon tetrachloride	CCl_4	Teratogenicity/carcinogenicity
−424	Hydroquinone		Oxidative stress
−423	Monocrotaline		Mutagenicity/carcinogenicity
−422	Vinyl chloride		Carcinogenicity
−421	Tributyltin chloride	TBT	Ship bottom paint/organotin
−420	Valproic acid		Antiepileptic
−419	Benzene		Carcinogenicity

TABLE 1—(*Continued*)

JCI No	Name	Abbreviation	Application/Target/Mechanism
−418	Acrylamide		Neurotoxin/carcinogenicity
−417	Hexachlorobenzene	BHC	Agricultural chemical/carcinogenicity
−346	2-Deoxyglucose	2-DG	Glycolytic pathway/glycosylation inhibitor
−325	Pentachlorophenol	PCP	Agricultural chemical/teratogenicity/carcinogenicity
−324	Aniline		Oxidative stress/methemoglobinemia/carcinogenicity
−323	Triazine		Agricultural chemical
−322	Edifenphos	EDDP	Agricultural chemical/antibiotics/choline esterase
−321	γ-1,2,3,4,5,6-Hexachlorocyclohexane	γ-BHC	Agricultural chemical/carcinogenicity
−320	Dichlorvos	DDVP	Agricultural chemical/teratogenicity/carcinogenicity
−319	*O*-Ethyl *O*-4-nitrophenyl phenylphosphonothioate	EPN	Agricultural chemical
−318	Cadmium chloride	$CdCl_2$	Teratogenicity/carcinogenicity
−317	Phenylmercury acetate	PMA	Fungicides/mutagenicity
−316	Mercaptoacetic acid		Synthetic intermediate
−315	1,3-Diphenylguanidine	DPG	Vulcanizing agent
−314	3,4,4′-Trichlorocarbanilide	TCC	Cosmetics/antibacterial agent
−313	3-Iodo-2-propynyl butylcarbamate	IPBC	Antibacterial agent
−311	2,3,3,3−2′,3′,3′,3′-Octachlorodipropylether	S-421	Agricultural chemical/antibacterial agent
−310	1,2-Benzisothiazolin-3-one	BIT	Antibacterial agent
−309	Isobornylthiocyanoacetate	IBTA	Antibacterial agent
−308	*p*-Chlorophenyl-3-iodopropargylformal	CPIP	Antibacterial agent
−307	Zinc butylxanthate	ZBX	Vulcanizing agent
−306	Polypropylene glycol	PG	Synthetic intermediate
−305	10,10′-Oxy-bis(phenoxyarsine)	OBPA	Antibacterial agent
−296	Snake venom from *Naja naja kaouthia*	SV-NNK	Snake venom
−295	Snake venom from *Naja nigricollis*	SV-NN	Snake venom
−294	2,5-di(*tert*-butyl)-1,4-Hydroquinone	DTBHQ	Oxidative stress
−293	Ibotenic Acid		Mushroom toxin/neurotoxin
−292	*N*-Methy-4-phenyl-1,2,3,6-tetrahydropyridine	MPTP	Neurotoxin
−289	Tetrodotoxin		Natural product/Na^+ channel inhibitor
−288	ICI 182,780		Estrogen antagonist
−275	Benzophenone		Agricultural chemical
−274	1,2-Dibromo-3-chloropropane	DBCP	Antibacterial agent/insecticide/carcinogenicity
−273	Zineb		Agricultural chemical
−272	Dieldrin		Insecticide
−271	Hexachlorobenzene	HCB	Antibacterial agent/carcinogenicity
−270	Ziram		Antibacterial agent/vulcanizing agent
−269	Chlordane		Insecticide/carcinogenicity
−268	4,4′-Dichlorodiphenyltrichloroethane	p,p′-DDT	Insecticide/carcinogenicity/teratogenicity
−267	Bisphenol A	BPA	Estrogenic
−266	17-β-Estradiol	E2	Estrogenic
−265	Diethylstilbestrol	DES	Estrogenic
−261	Paraquat		Agricultural chemical/oxidative stress
−247	Ouabain		Cardiac glycosides
−245	Okadaic acid		Natural product/PP1, PP2A inhibitor
−242	Antimycin A1		Agricultural chemical
−232	Digoxin		Cardiac glycosides
−201	OH-Flutamide		Flutamide derivative/androgen antagonist
−200	Flutamide		Anticancer drugs/androgen antagonist
−185	30% H_2O_2		Oxidative stress
−182	*N*-Acetyl-L-cysteine	NAC	Super oxyside scavenger
−181	L-Ascorbic acid		Food constituent
−179	Dopamine		Neurotransmitter
−177	Caffeine		Food constituent
−168	Cycloheximide		Protein synthesis inhibitor
−144	4-Hydroxyphenylretinamide	4-HPR	RAR
−137	Indomethacin		COX inhibitor
−99	SN-38		Irinotecan derivative/Topo I
−96	Toremifene		Anticancer drugs/estrogen antagonist
−95	Tamoxifen		Anticancer drugs/estrogen antagonist
−63	Cyclosporin A		Anticancer drugs/helper T cell
−46	HCFU		Anticancer drugs/antimetabolite(pyrimidine)
−36	Docetaxel		Anticancer drugs/tubulin
−35	Paclitaxel		Anticancer drugs/tubulin
−34	Colchicine		Antipodagric/tubulin
−33	Cisplatin		Anticancer drugs/DNA cross linker
−32	Carboplatin		Anticancer drugs/DNA cross linker
−31	Irinotecan		Anticancer drugs/Topo I
−30	Camptothecin	CPT	Anticancer drugs/Topo I
−24	Methotrexate		Anticancer drugs/DHFR
−19	Vincristine		Anticancer drugs/tubulin
−18	Vinblastine		Anticancer drugs/tubulin
−16	Mitomycin-C	MMC	Anticancer drugs/DNA alkylator
−9	Tegafur		Anticancer drugs/antimetabolite(pyrimidine)
−8	5-Fluorouracil	5-FU	Anticancer drugs/antimetabolite(pyrimidine)
−5	Cytarabine		Anticancer drugs/antimetabolite(pyrimidine)
−4	Nitrogen mustard		Anticancer drugs/DNA alkylator

RAR, retinoic acid receptor; RXR; retinoid X receptor.

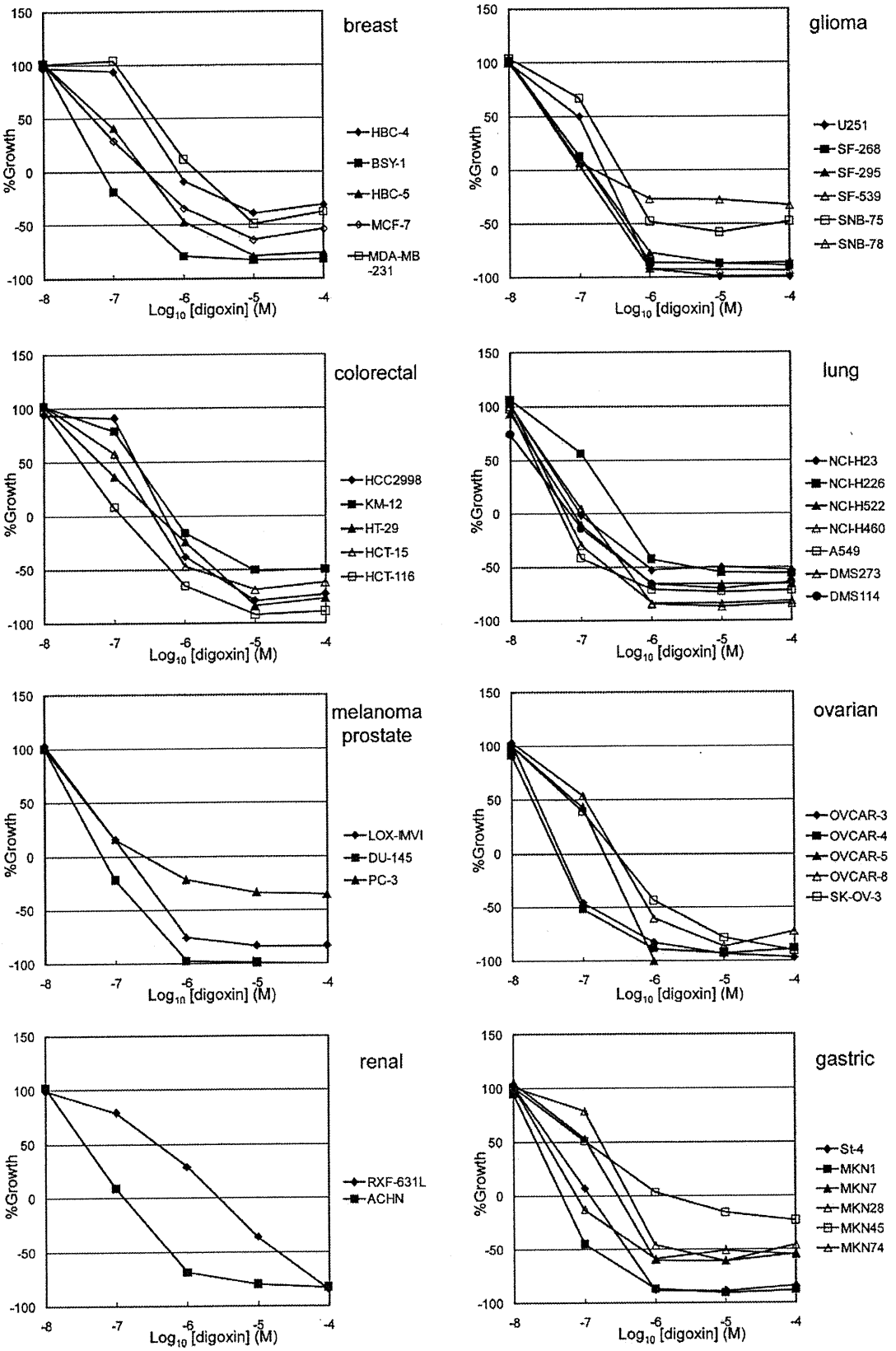

Fig. 1. Dose response curves of digoxin against growth of JFCR-39 cells. The *x*-axis represents concentration of digoxin and the *y-axis* represents percentage growth. The GI50 represents the concentration required to inhibit cell growth by 50% compared with untreated controls.

the standard anticancer drugs using the COMPARE algorithm (Yamori et al., 1999). We have used this system successfully and demonstrated that the molecular targets of the novel chemicals MS-274, FJ5002, and ZSTK474 were topoisomerases I and II (Yamori et al., 1999), telomerase (Naasani et al., 1999), and phosphatidylinositol 3-kinase (Yaguchi et al., 2006), respectively. Several other interesting studies, based on a panel of cancer cells, classified anticancer drugs according to their action mechanisms or molecular targets by cluster analysis of their GI50 values (Weinstein et al., 1992, 1997; Dan et al., 2002). Correlation analysis has also been used to explore the genes associated with the sensitivity of the cells in the panel to anticancer drugs (Scherf et al., 2000; Okutsu et al., 2002; Zembutsu et al., 2002; Nakatsu et al., 2005).

In this study, we have examined the potential of the JFCR39 system in classifying various chemicals, and predicted their action mechanisms. For this purpose, we have determined the fingerprints of 130 different types of chemicals including toxic chemicals, pesticides, drugs and synthetic intermediates, and then classified these chemicals according to the cluster analysis of their fingerprints.

Materials and Methods

Cell Lines and Cell Cultures. The panel of human cancer cell lines has been described previously (Yamori et al., 1999; Dan et al., 2002) and consists of the following 39 human cancer cell lines: lung cancer, NCI-H23, NCI-H226, NCI-H522, NCI-H460, A549, DMS273, and DMS114; colorectal cancer, HCC-2998, KM-12, HT-29, HCT-15, and HCT-116; gastric cancer, MKN-1, MKN-7, MKN-28, MKN-45, MKN-74, and St-4; ovarian cancer, OVCAR-3, OVCAR-4, OVCAR-5, OVCAR-8, and SK-OV-3; breast cancer, BSY-1, HBC-4, HBC-5, MDA-MB-231, and MCF-7; renal cancer, RXF-631L and ACHN; melanoma, LOX-IMVI; glioma, U251, SF-295, SF-539, SF-268, SNB-75, and SNB-78; and prostate cancer, DU-145 and PC-3. All cell lines were cultured in RPMI 1640 medium (Nissui Pharmaceutical, Tokyo, Japan) with 5% fetal bovine serum, penicillin (100 units/ml), and streptomycin (100 μg/ml) at 37°C under 5% CO_2.

Determination of Cell Growth Inhibition Profiles. Growth inhibition experiments were performed to assess the sensitivity of the cells to various chemicals as described before (Yamori et al., 1999; Dan et al., 2002). Growth inhibition was measured by determining the changes in the amounts of total cellular protein after 48 h of chemical treatment using a sulforhodamine B assay. For each chemical, the growth assay was performed using a total of five different concentrations of the chemical (for example, 10^{-4}, 10^{-5},

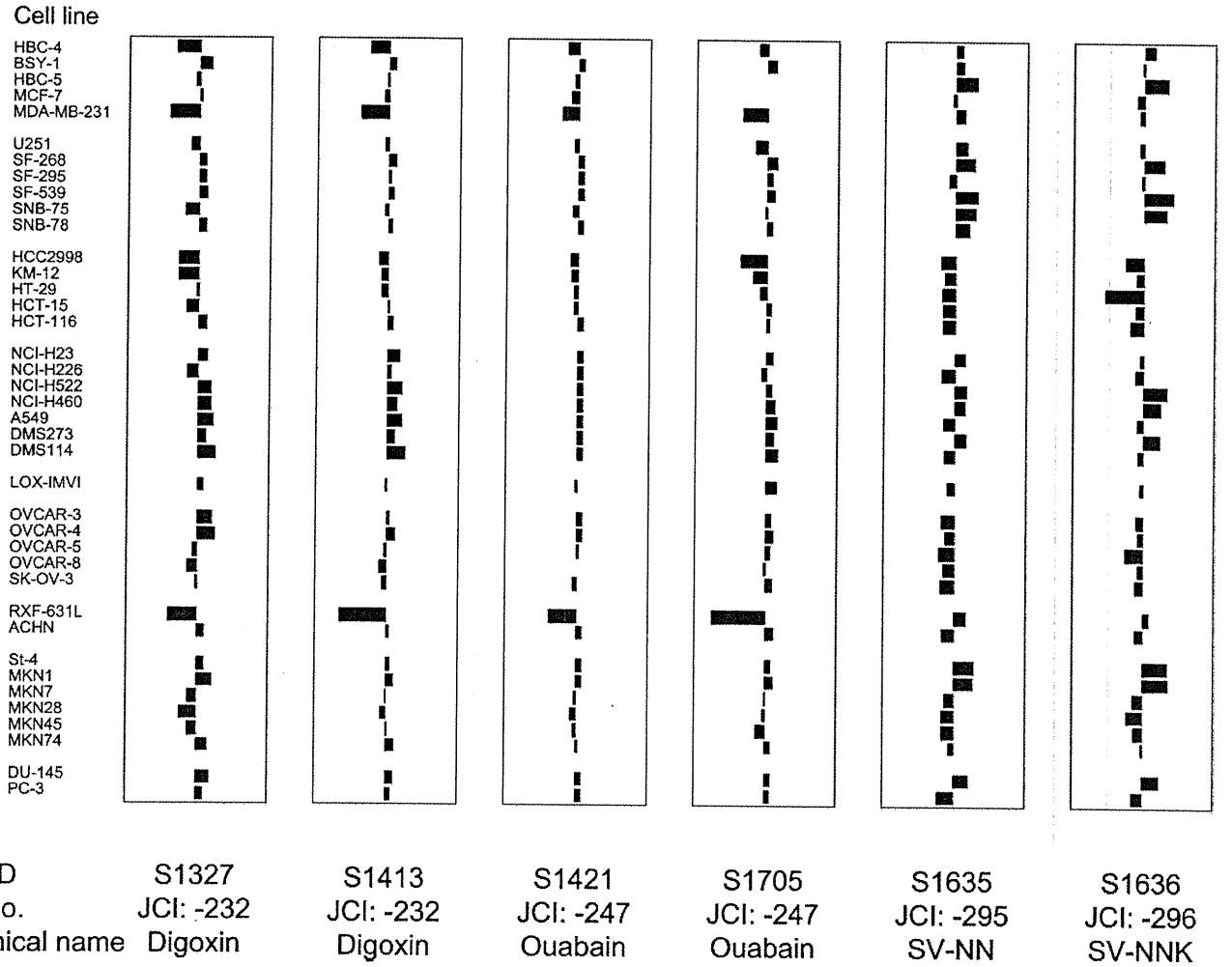

Fig. 2. Fingerprints of digoxin, ouabain, SV-NN, and SV-NNK. Fingerprint shows the differential growth inhibition pattern of the cells in the JFCR-39 panel against the test chemical. The *X*-axis represents relative value of GI50; $(-1) \times$ (log GI50 − MG-MID); MG-MID is the mean value of the log GI50. Zero means the mean GI50 and one means the GI50 value is 10-fold more sensitive than the mean GI50. Exp-ID and JCI numbers are the ID for the experiment and ID for the chemical, respectively, in our database.

10^{-6}, 10^{-7}, and 10^{-8} M) and one negative control. All assays were performed in duplicate. This GI50 calculation method is well established and reliable through anticancer drug screen using NCI60 as well as JFCR39 (Paull et al., 1989; Yamori et al., 1999; Yamori, 2003). At each test concentration, the percentage growth was calculated using the following seven absorbance measurements: growth at time 0 (T0), growth of the control cells (C), and test growth in the presence of five different concentrations (T) of a drug. The percentage growth inhibition was calculated as: % growth = $100 \times [(T - T0)/(C - T0)]$ when $T \geq T0$, and % growth = $100 \times [(T - T0)/T]$ when $T < T0$. The GI50 values, which represent 50% growth inhibition concentration, were calculated as $100 \times [(T - T0)/(C - T0)] = 50$. When the GI50 of a chemical could not be calculated, the highest used concentration was assigned as its GI50 value. Absolute values of GI50 were then log transformed for further analysis. We certified the accuracy of measured GI50 data by using reference control chemicals, such as mitomycin-C, paclitaxel, and SN-38, in every experiment and by checking the dose response curves.

Chemicals. Spironolactone, *para*-aminoazobenzene, *para*-cresidine, neostigmine bromide, *para*-dichlorobenzene, phenytoin, *ortho*-toluidine, imipramine, cobalt chloride, atrazine, propylthiouracil, (D,L)-thalidomide, carbon tetrachloride, hydroquinone, monocrotaline, vinyl chloride, tributyl-tin chloride, valproic acid, benzene, acrylamide, pentachlorophenol, aniline, 1,3-diphenylguanidine, polypropylene glycol, 10,10′-oxy-bis(phenoxyarsine), testosterone propionate, carbaryl, acephate, bisphenol A, 17-β-estradiol, diethylstilbestrol, and α-bungarotoxin were purchased from Wako (Tokyo, Japan). Snake venoms from *Agkistrodon halys blomhoffii*, *Trimeresurus flavoviridis*, *Crotalus atrox*, *Naja nigricollis*, and *Naja naja kaouthia* were purchased from Latoxan (Valence, France). 2-Aminomethylpyridine, 1*H*-1,2,4-triazole, 1*H*-1,2,3-triazole, 3,4,4′-trichlorocarbanilide, edifenphos, dichlorvos, *O*-ethyl *O*-4-nitrophenyl phenylphosphonothioate, 2,4-dinitrophenol, *N*-methylaniline, 1,2-dichloro-3-nitrobenzene, 4-ethylnitrobenzene, 2-vinylpyridine, 3-amino-1*H*-1,2,4-triazole, *N*-ethyl-*N*-nitrosourea, 5-aza-2′- deoxycytidine, ethynyl estradiol, 3-methylcholanthrene, phenobarbital, acetaminophen, isoniazid, capsaicin, *N*-deacetyl-*N*-methylcolchicine (Colcemid), 2.4-dinitrochlorobenzene, and dexamethasone were from Sigma Chemicals (St. Louis, MO). Methoprene acid, methoprene, all-*trans* retinoic acid, and 9-cis retinoic acid were from BIOMOL International L.P. (Plymouth Meeting, PA). Levothyroxine was from MP Biomedicals (Irvine, CA). 3-Iodo-2-propynyl butylcarbamate was from Olin Japan Inc. (Tokyo, Japan), *p*-chlorophenyl-3-iodopropargylformal was from Nagase ChemteX (Osaka, Japan), and 2,3,3,3–2′,3′,3′,3′-octachlorodipropylether was from Sankyo Chemical Industries, Ltd. (Tokyo, Japan). 1,2-Benzisothiazolin-3-one was from Riverson (Osaka, Japan), zinc butylxanthate was from Ouchishinko Chemical Industrial Co., Ltd. (Tokyo, Japan), and 4-amino-2,6-dichlorophenol was from Tokyo Kasei Kogyo Co. Ltd. (Tokyo, Japan).

Hierarchical Clustering. Hierarchical clustering analysis was carried out using the average linkage method and the "GeneSpring" software (Silicon Genetics, Inc., Redwood, CA). Pearson correlation coefficients were used to determine the degree of similarity.

Results

Sensitivity of JFCR39 to Chemicals. Sensitivity of the JFCR39 panel of cells to 130 chemicals was determined as described under *Materials and Methods*. Table 1 summarizes

TABLE 2
Log_{10} GI50 values of chemicals for each cell line in the JFCR-39 panel
Hi-conc means the highest concentration of the test chemical used. When the growth inhibition was over 50% at the Hi-Conc, GI_{50} was assigned the Hi-Conc value.

Exp-ID	S3416	S3415	S3413	S3245	S3117	S3414	S3118	S3246	S3125	S3124	S3123	S1636	S1635	S1634	S1718
JCI No	−687	−686	−559	−559	−559	−560	−560	−560	−567	−566	−565	−296	−295	−294	−294
Name or Abbr.	TTNPB	13-*cis*	9-*cis*			ATRA			SV-TF	SV-CA	SV-AHB	SV-NNK	SV-NN	DTBHQ	
Hi-Conc.	−4	−4	−4	−4	−4	−4	−4	−4	−4	−4	−4	−4	−4	−4	−4
HBC-4	−4.76	−4.00	−4.53	−4.40	−4.43	−4.42	−4.41	−4.41	−5.87	−5.80	−5.66	−7.25	−7.31	−4.72	−4.80
BSY-1	−4.78	−4.16	−4.60	−4.73	−4.73	−4.69	−4.70	−4.81	−6.31	−6.06	−5.76	−6.93	−7.34	−5.07	−4.93
HBC-5	−4.80	−4.41	−4.56	−4.57	−4.61	−4.61	−4.47	−4.51	−6.98	−6.45	−5.73	−7.64	−7.72	−4.89	−4.78
MCF-7	−4.73	−4.35	−4.40	−4.39	−4.48	−4.48	−4.54	−4.66	−5.87	−5.78	−5.68	−6.77	−7.08	−5.29	−5.25
MDA-MB-231	−4.75	−4.21	−4.70	−4.55	−4.69	−4.63	−4.53	−4.65	−5.90	−5.86	−5.84	−6.84	−7.39	−5.52	−5.30
U251	−4.77	−4.14	−4.61	−4.51	−4.61	−4.57	−4.45	−4.63	−6.45	−5.76	−5.70	−6.85	−7.44	−4.96	−5.11
SF-268	−4.75	−4.00	−4.24	−4.55	−4.40	−4.47	−4.48	−4.76	−5.90	−5.79	−5.70	−7.53	−7.67	−4.77	−4.81
SF-295	−4.80	−4.29	−4.54	−4.66	−4.60	−4.59	−4.48	−4.57	−6.19	−5.80	−5.74	−6.89	−6.97	−4.87	−4.97
SF-539	−4.95	−4.35	−4.75	−4.80	−4.79	−4.80	−4.71	−4.76	−6.39	−5.96	−5.81	−7.79	−7.75	−4.79	−4.86
SNB-75	−5.31	−5.28	−5.13	−5.19		−4.71	−4.69	−4.87	−6.41	−6.33	−5.93	−7.60	−7.70	−4.67	−4.80
SNB-78	−4.77	−4.25	−4.69	−4.78	−4.86	−4.49	−4.70	−4.68	−6.19	−6.00	−5.95	−6.97	−7.53	−4.75	−4.75
HCC2998	−4.68	−4.00	−4.48	−4.61	−4.62	−4.55	−4.62	−4.76	−5.91	−5.75	−5.67	−6.47	−6.77	−4.82	−4.75
KM-12	−4.70	−4.00	−4.46	−4.51	−4.48	−4.51	−4.47	−4.58	−5.93	−5.80	−5.65	−6.77	−6.87	−4.74	−4.77
HT-29	−4.73	−4.00	−4.47	−4.53	−4.50	−4.60	−4.52	−4.56	−5.90	−5.80	−5.56	−5.89	−6.78	−4.80	−4.89
HCT-15	−4.72	−4.25	−4.45	−4.49	−4.48	−4.52	−4.57	−4.53	−5.88	−5.76	−5.57	−6.73	−6.82	−4.72	−4.77
HCT-116	−4.77	−4.07	−4.67	−4.59	−4.67	−4.71	−4.61	−4.64	−6.46	−6.10	−5.77	−6.58	−6.82	−4.98	−5.13
NCI-H23	−4.74	−4.00	−4.47	−4.60	−4.59	−4.61	−4.55	−4.63	−6.11	−5.75	−5.72	−6.86	−7.42	−4.76	−4.90
NCI-H226	−4.72	−4.00	−4.61	−4.68	−4.78	−4.80	−4.54	−5.48	−5.95	−5.81	−5.76	−6.73	−6.78	−4.89	−4.91
NCI-H522	−4.72	−4.45	−4.68	−4.82	−4.77	−4.71	−4.71	−4.68	−6.45	−5.99	−5.78	−7.62	−7.46	−5.37	−5.37
NCI-H460	−4.70	−4.00	−4.55	−4.63	−4.58	−4.68	−4.55	−4.49	−5.96	−5.82	−5.72	−7.44	−7.42	−4.84	−4.84
A549	−4.79	−4.00	−4.72	−4.77	−4.78	−4.70	−4.62	−4.53	−5.91	−5.79	−5.71	−6.80	−6.83	−4.83	−4.87
DMS273	−4.57	−4.21	−4.50	−4.62	−4.55	−4.57	−4.51	−4.49	−6.20	−5.81	−5.72	−7.43	−7.44	−4.91	−4.98
DMS114	−4.77	−4.16	−4.33	−4.62	−4.49	−4.51	−4.53	−4.61	−6.66	−6.33	−5.77	−6.83	−6.88	−5.12	−5.21
LOX-IMVI	−4.77	−4.69	−4.68	−4.66	−4.70	−4.77	−4.74	−4.74	−6.75	−6.59	−5.76	−6.86	−6.94	−5.05	−5.15
OVCAR-3	−4.77	−4.38	−4.56	−4.67	−4.72	−4.64	−4.62	−4.71	−6.61	−6.13	−5.89	−6.77	−6.79	−4.89	−4.86
OVCAR-4	−4.72	−4.05	−4.63	−4.64	−4.64	−4.58	−4.39	−4.54	−6.73	−6.23	−5.80	−6.82	−6.90	−5.13	−4.90
OVCAR-5	−4.75	−4.00	−4.33	−4.39	−4.42	−4.44	−4.34	−4.44	−5.92	−5.74	−5.67	−6.46	−6.71	−5.22	−5.26
OVCAR-8	−4.75	−4.23	−4.50	−4.53	−4.59	−4.66	−4.67	−4.70	−5.95	−5.77	−5.69	−6.82	−6.84	−4.64	−4.70
SK-OV-3	−4.79	−4.00	−4.49	−4.51	−4.81	−4.52	−4.54	−4.50	−5.76	−5.64	−4.91	−6.75	−6.76	−4.64	−4.74
RXF-631L	−4.77	−4.00	−4.54	−4.58	−4.60	−4.72	−4.63	−4.61	−5.91	−5.80	−5.59	−7.13	−7.46	−4.81	−4.84
ACHN	−4.73	−4.00	−4.56	−4.66	−4.56	−4.50	−4.40	−4.76	−5.90	−5.79	−5.73	−6.74	−6.80	−4.71	−4.83
St-4	−4.74	−4.00	−4.42	−4.54	−4.65	−4.53	−4.49	−4.57	−5.91	−5.81	−5.76	−7.65	−7.70	−4.68	−4.75
MKN1	−4.75	−4.33	−4.56	−4.63	−4.62	−4.56	−4.45	−4.48	−6.15	−5.81	−5.78	−7.67	−7.68	−4.59	−4.81
MKN7	−4.78	−4.40	−4.68	−4.59	−4.70	−4.73	−4.56	−4.65	−6.29	−5.85	−5.76	−6.70	−6.90	−4.79	−4.84
MKN28	−4.71	−4.28	−4.56	−4.59	−4.59	−4.65	−4.56	−4.60	−6.10	−5.93	−5.68	−6.51	−6.81	−4.72	−4.89
MKN45	−4.72	−4.00	−4.51	−4.41	−4.46	−4.73	−4.41	−4.43	−6.06	−5.90	−5.69	−6.71	−6.82	−4.71	−4.87
MKN74	−4.74	−4.40	−4.61	−4.63	−4.61	−4.73	−4.68	−4.67	−5.97	−5.92	−5.61	−6.92	−7.00	−5.10	−5.42
DU-145	−4.68	−4.00	−4.25	−4.78	−4.41	−4.42	−4.44	−4.54	−6.08	−5.82	−5.75	−7.43	−7.55	−4.59	−5.02
PC-3	−4.74	−4.00	−4.58	−4.65	−4.48	−4.74	−4.39	−4.51	−5.83	−5.77	−5.61	−6.67	−6.69	−4.89	−4.74

abbreviations, applications, targets, and known mechanisms of 130 chemicals and 21 anticancer drugs. Approximately 15% of the chemicals were assessed twice or more. Approximately 40% of the chemicals tested had little effect on the growth of cells in the JFCR39 panel. However, the rest of the chemicals significantly inhibited the cell growth across the JFCR39 panel. For example, Fig. 1 shows the dose response curves of the cells in the JFCR39 panel against digoxin. The concentration at which the cell growth is inhibited by 50% represents GI50. Figure 2 shows the fingerprints of four chemicals [digoxin, ouabain, snake venom from *N. nigricollis* (SV-NN), and snake venom from *N. naja kaouthia* (SV-NNK)], which differentially inhibited the growth of cells in the JFCR39 panel; these fingerprints were drawn based on a calculation using a set of GI50s and clearly represented the GI50 pattern. These results were highly reproducible in that the Pearson correlation coefficient of the duplicate experiments for digoxin was 0.839 ($p < 0.001$) and that for ouabain was 0.864 ($p < 0.001$). It is noteworthy that, digoxin and ouabain, both of which are cardiac glycosides and inhibit Na-K ATPase, showed similar fingerprints. The fingerprints of SV-NNK and SV-NN, which belong to the elapidae, known as cobras, were also similar, but were different from the fingerprints of digoxin and ouabain. Table 2 summarizes only a portion of the GI50 values from 160 experiments involving 130 chemicals and 42 experiments involving 21 anticancer drugs. GI50 values from all experiments are described in the Supplemental Data (Table S1). All these data were stored in a chemosensitivity database and used for further analysis.

Classification of the Chemicals by Hierarchical Clustering. Sixty-nine chemicals were selected for further analysis based on the following criteria: 1) GI50 values for the test chemical can be determined for at least 10 cell lines in the JFCR39 panel, and 2) the range of log GI50 for the test chemical is more than 0.6, suggesting differential growth inhibition. We analyzed the GI50 values of these 69 chemicals and 20 anticancer drugs by hierarchical clustering analysis (Fig. 3). We found approximately 12 clusters (threshold: $r = 0$, Fig. 3, clusters A–L), which were further divided into 49 subclusters (threshold: $r = 0.408$, Fig. 3, clusters A1–L6).

Analysis of Clusters. Most anticancer drugs we have tested belonged either to cluster A or cluster H, depending on their modes of action (Dan et al., 2002). The targets of the anticancer drugs belonging to the cluster A were related to DNA (Topo I, antimetabolite of pyridine, DNA alkylator) and the target of the anticancer drugs belonging to the cluster H was tubulin. We presently found that cisplatin exceptionally belonged to cluster F2, not cluster A, although it is known to cross-link DNA strands (Jamieson and Lippard, 1999; Wong and Giandomenico, 1999). We were also able to precisely group the clusters into several subclusters having similar characteristics. For example, the cardiac glycosides digoxin and ouabain were grouped in one cluster (cluster F3). SV-

S3243	S3244	S1534	S3237	S3238	S1525	S3236	S1928	S1421	S1705	S1327	S1413	S1413	S3408	S3409	S2421
−599	−599	−270	−270	−270	−261	−261	−261	−247	−247	−232	−232	−232	−421	−421	−421
Thiram		Ziram			Paraquat			Ouabain		Digoxin			TBT		
−4	−4	−4	−4	−4	−4	−3	−4	−4	−6	−4	−4	−4	−4	−4	−4
−4.71	−4.79	−5.80	−5.73	−5.70	−4.00	−3.61	−4.00	−7.54	−7.28	−6.57	−6.96	−6.96	−6.79	−6.77	−6.72
−6.97	−7.12	−6.85	−6.76	−6.60	−4.00	−4.45	−4.51	−8.00	−7.76	−7.58	−7.68	−7.68	−7.03	−7.01	−6.83
−7.41	−7.66	−7.18	−7.47	−7.47	−4.68	−4.70		−7.76	−7.51	−7.15	−7.44	−7.44	−6.76	−6.88	−6.83
−4.77	−4.80	−6.00	−5.84	−5.83	−4.06	−3.72	−4.00	−7.64	−7.51	−7.29	−7.39	−7.39	−6.86	−6.84	−6.79
−4.66	−4.68	−5.64	−5.75	−5.63	−4.00	−3.57	−4.00	−7.40	−6.81	−6.41	−6.72	−6.72	−6.83	−6.81	−6.70
−4.75	−4.78	−5.71	−5.79	−5.82	−4.00	−3.69	−4.00	−7.75	−7.16	−7.01	−7.40	−7.40	−6.79	−6.77	−6.72
−4.86	−4.96	−5.74	−5.83	−7.01	−4.00	−4.08	−4.00	−8.00	−7.77	−7.42	−7.70	−7.70	−6.84	−6.85	−6.71
−4.77	−4.89	−5.71	−5.70	−5.79	−4.47	−4.37	−4.20	−8.00	−7.64	−7.42	−7.55	−7.55	−6.75	−6.73	−6.76
−4.75	−4.88	−5.73	−5.75	−5.77	−4.00	−4.03	−4.00	−8.00	−7.70	−7.46	−7.63	−7.63	−6.77	−6.72	−6.67
−4.71	−4.96	−5.79	−5.92	−5.80	−4.00	−3.94	−4.00	−7.70	−7.45	−6.86	−7.40	−7.40	−6.99	−6.95	−7.05
−4.70	−4.78	−5.69	−5.64	−5.69	−4.00	−3.78	−4.00	−7.98	−7.64	−7.45	−7.60	−7.60	−6.72	−6.79	−6.70
−4.82	−4.69	−5.76	−5.79	−5.81	−4.00	−3.70	−4.00	−7.64	−6.77	−6.68	−7.25	−7.25	−6.77	−6.79	−6.72
−4.80	−4.80	−5.43	−5.74	−5.73	−4.00	−3.58	−4.00	−7.67	−7.12	−6.69	−7.34	−7.34	−7.00	−6.98	−6.74
−4.68	−4.85	−5.75	−5.77	−5.76	−4.10	−4.03	−4.07	−7.75	−7.31	−7.20	−7.34	−7.34	−6.89	−6.84	−6.66
−4.68	−4.75	−5.70	−5.72	−5.83	−4.00	−3.64	−4.00	−7.74	−7.63	−6.92	−7.54	−7.54	−6.88	−6.84	−6.70
−4.72	−4.72	−5.74	−5.68	−5.77	−4.00	−3.60	−4.00	−8.00	−7.57	−7.47	−7.62	−7.62	−6.90	−6.85	−6.74
−4.69	−4.78	−5.96	−5.85	−5.84	−4.19	−4.18	−4.00	−8.00	−7.67	−7.50	−7.84	−7.84	−6.90	−6.85	−6.76
−6.33	−6.74	−5.63	−5.96	−6.12	−4.41	−4.41	−4.00	−8.00	−7.37	−6.93	−7.61	−7.61	−6.99	−6.91	−6.74
−7.49	−7.50	−7.44	−7.66	−8.00	−4.49	−4.71	−4.59	−8.00	−7.64	−7.59	−7.91	−7.91	−6.83	−6.80	−6.25
−6.14	−6.16	−6.30	−6.10	−6.15	−4.30	−4.45	−4.37	−8.00	−7.74	−7.60	−7.77	−7.77	−6.98	−6.98	−6.56
−4.84	−4.82	−5.97	−5.91	−5.91	−4.49	−4.49	−4.41	−8.00	−7.80	−7.66	−7.91	−7.91	−6.82	−6.87	−6.73
−6.64	−6.58	−6.43	−6.84	−6.82	−4.25	−4.43	−4.30	−8.00	−7.71	−7.48	−7.72	−7.72	−6.74	−6.75	−6.70
−7.18	−7.39	−7.37	−7.38	−7.43	−4.50	−4.63	−4.27	−8.00	−7.84	−7.73	−8.00	−8.00	−7.11	−7.12	−7.02
−4.68	−4.71	−5.66	−5.71	−5.70	−4.00	−3.51	−4.00	−7.80	−7.80	−7.39	−7.46	−7.46	−6.93	−6.94	−6.76
−4.86	−6.25	−6.07	−6.35	−6.32	−4.00	−4.46	−4.28	−8.00	−7.66	−7.64	−7.59	−7.59	−6.80	−6.82	−6.74
−4.77	−6.67	−5.90	−5.91	−5.87	−4.00	−4.21	−4.48	−8.00	−7.71	−7.71	−7.72	−7.72	−6.91	−7.20	−6.80
−4.90	−6.00	−6.11	−6.91	−6.74	−4.00	−3.98	−4.00	−7.89	−7.62	−7.12	−7.42	−7.42	−6.90	−6.93	−6.75
−4.62	−4.74	−5.59	−5.68	−5.67	−4.00	−3.84	−4.00	−7.85	−7.44	−6.97	−7.29	−7.29	−6.73	−6.67	−6.57
−4.39	−4.38	−4.92	−5.49	−5.53	−4.00	−3.39	−4.00	−7.74	−7.67	−7.18	−7.38	−7.38	−6.80	−6.77	−6.68
−4.75	−4.65	−5.57	−5.63	−5.60	−4.00	−3.60	−4.00	−7.10	−6.00	−6.42	−6.20	−6.20	−6.78	−6.76	−6.68
−4.52	−4.60	−5.64	−5.68	−5.69	−4.00	−3.51	−4.00	−8.00	−7.72	−7.44	−7.59	−7.59	−6.78	−6.77	−6.76
−4.59	−4.72	−5.99	−5.73	−5.81	−4.00	−3.58	−4.00	−8.00	−7.65	−7.45	−7.60	−7.60	−6.80	−6.80	−6.72
−4.80	−4.85	−6.82	−5.84	−5.92	−4.41	−4.61	−4.48	−8.00	−7.72	−7.68	−7.72	−7.72	−7.25	−7.15	−6.87
−4.79	−4.82	−6.56	−5.84	−5.82	−4.08	−4.29	−4.32	−7.80	−7.48	−6.98	−7.47	−7.47	−7.34	−7.07	−6.86
−7.18	−7.21	−5.82	−7.09	−7.13	−4.00	−4.40	−4.18	−7.70	−7.42	−6.77	−7.37	−7.37	−6.84	−6.82	−6.87
−6.65	−6.71	−6.05	−7.18	−6.86	−4.00	−4.29	−4.35	−7.77	−7.25	−6.99	−7.52	−7.52	−6.96	−6.97	−6.87
−7.05	−7.08	−6.35	−5.86	−7.05	−4.00	−4.47	−4.06	−7.91	−7.65	−7.55	−7.74	−7.74	−6.97	−7.37	−7.05
−4.47	−4.70	−5.68	−5.68	−5.65	−4.00	−3.57	−4.00	−8.00	−7.64	−7.59	−7.71	−7.71	−6.90	−6.89	−6.70
−4.42	−4.77	−5.61	−5.53	−5.56	−4.00	−3.64	−4.37	−8.00	−7.62	−7.41	−7.62	−7.62	−6.77	−6.78	−6.73